Nature. Author manuscript; available in PMC 2015 July 01.

Published in final edited form as:
Nature. 2015 January 1; 517(7532): 94–98. doi:10.1038/nature14019.

A PP1/PP2A phosphatase relay controls mitotic progression

Agnes Grallert[#1], **Elvan Boke**[#1,‡], **Anja Hagting**[3], **Ben Hodgson**[1], **Yvonne Connolly**[2], **John. R. Griffiths**[2], **Duncan L. Smith**[2], **Jonathon Pines**[3], and **Iain M. Hagan**[1]

[1]Cell Division Group, CRUK Manchester Institute, University of Manchester, Wilmslow Road, Manchester, M20 4BX, UK

[2]Biological Mass Spectrometry, CRUK Manchester Institute, University of Manchester, Wilmslow Road, Manchester, M20 4BX, UK

[3]The Gurdon Institute, University of Cambridge, Cambridge CB2 1QN, UK

[#] These authors contributed equally to this work.

Summary

The widespread reorganisation of cellular architecture in mitosis is achieved through extensive protein phosphorylation, driven by the coordinated activation of a mitotic kinase network and repression of counteracting phosphatases. Phosphatase activity must subsequently be restored to promote mitotic exit. Although Cdc14 phosphatase drives this reversal in budding yeast, Protein Phosphatase 1 (PP1) and Protein Phosphatase 2A (PP2A) activities have each been independently linked to mitotic exit control in other eukaryotes[1-6]. We now describe a mitotic phosphatase relay in which PP1 reactivation is required for the reactivation of both PP2A-B55 and PP2A-B56 to coordinate mitotic progression and exit in fission yeast. The staged recruitment of PP1 to the regulatory subunits of PP2A-B55 and PP2A-B56 holoenzymes sequentially activates each phosphatase. The pathway is blocked in early mitosis because Cdk1-Cyclin B inhibits PP1 activity but declining Cyclin B levels later in mitosis permit PP1 to auto-reactivate[1,7-10]. PP1 first reactivates PP2A-B55; this enables PP2A-B55, in turn, to promote the reactivation of PP2A-B56 by dephosphorylating a PP1 docking site in PP2A-B56, thereby promoting the recruitment of PP1. PP1 recruitment to human, mitotic, PP2A holoenzymes and the sequences of these conserved PP1 docking motifs[11,12] suggest that PP1 regulates PP2A-B55 and PP2A-B56 activities in a variety of signalling contexts throughout eukaryotes.

Correspondence and requests for materials should be addressed to: **IMH:**Iain.Hagan@cruk.manchester.ac.uk.
[‡]Present Address: Department of Systems Biology, Harvard Medical School, Boston, Massachusetts, USA

Author Contributions

Initial identification, validation and timing of $PP1^{Dis2}$-$B55^{Pab1}$/$B56^{Par1}$ association by two hybrid and co-immunoprecipitation, specificity and timing of $PP1^{Dis2}$.T316 phospho-recognition, phosphomapping of $B56^{Par1}$ (with DS and YC) and generation of some mutant alleles EB. Fig 4d EB. All other data presented except for Figs 4k, Extended Data 5c and 9b-d were generated and largely devised by AG. Data for ED5c, AG, YC, DS and JG. Molecular biology and background work for human two hybrid assays and generation human vectors BH. IH devised the work in Figs 1c, 2a,c,f, 4d with EB and remainder with AG. Design and execution of human work and gel filtration AH and JP.

The authors declare that they have no competing financial interests.

Europe PMC Funders Author Manuscripts

Cdk1/Cyclin B phosphorylation of a conserved site in the C terminus of PP1 depresses PP1 activity at mitotic commitment[1,7-10]. Declining Cdk1/Cyclin B levels then allow the compromised PP1 to dephosphorylate itself to promote a return to full activity[1,7]. Of the two fission yeast PP1 enzymes, $PP1^{Sds21}$ and $PP1^{Dis2}$, only $PP1^{Dis2}$ harbours the conserved inhibitory phosphorylation site[2,9] (Extended Data Figure 1a). *In vitro* $PP1^{Dis2}$ activity assays re-capitulated previous observations that T316 phosphorylation by Cdk1-Cyclin B depressed activity (Figure 1a; Extended Data Figure 1b, c)[1,7,9]. Mutating T316 to aspartic acid to mimic phosphorylation reduced the activity to a similar degree to phosphorylation by Cdk1-Cyclin B (Figure 1a; Extended Data Figure 1c). Replacement of $PP1^{dis2+}$ with a $PP1^{dis2}$*.316A* allele increased $PP1^{Dis2}$ levels, whereas they were reduced in $PP1^{dis2}$*.316D* (Figure 1b), indicating that phosphorylated T316 might act as a phospho-degron. Since this interpretation conflicted with reports of stable $PP1^{Dis2}$ levels throughout mitosis[10,13], we monitored $PP1^{Dis2}$ levels with both low and high antibody dilutions as size selected cells synchronously transited the cell cycle. A transient reduction in $PP1^{Dis2}$ levels as T316 phosphorylation peaked (Figure 1c) was blocked when proteosome function was inhibited (Extended Data Figure 1e). Consistently, $PP1^{Dis2}$ levels were persistently low in $PP1^{dis2}$*.316D* and persistently high in $PP1^{dis2}$*.316A* (Figure 1c; Extended Data Figure 1f,g) indicating that phosphorylation of T316 by Cdk1-Cyclin B both reduces $PP1^{Dis2}$ levels and inhibits its phosphatase activity.

PP2A holoenzymes combine a catalytic and scaffolding subunit with one of four regulatory B subunits[14], of which PP2A-B55 and PP2A-B56 have been linked to mitotic control[3-5,15,16]. We noticed that the B55 and B56 regulatory subunits had highly conserved PP1 docking site consensus motifs (RVxF/RxVxF)[12] (Figure 2a). The *S. pombe* genome encodes one B55 ($B55^{Pab1}$) and two B56 subunits ($B56^{Par1}$ and $B56^{Par2}$)[17,18], and we found that both $B55^{Pab1}$ and $B56^{Par1}$ associated with $PP1^{Dis2}$ in immunoprecipitation assays (Figure 2b; Extended Data Figure 2a-d). $B56^{Par1}$ also bound $PP1^{Dis2}$ in a yeast two-hybrid assay (Extended Data Figure 3), and the functional replacement of the PP1 docking site of the morphogenesis regulator Wsh3/Tea4[19] by the SKEVLF motif of $B56^{Par1}$ confirmed its ability to recruit $PP1^{Dis2}$ (Extended Data Figure 4a-d). The interaction between $PP1^{Dis2}$ and $B55^{Pab1}$ was abolished by mutating the PP1 docking consensus motif (Figure 2b; Extended Data Figure 2a). No association was found between $PP1^{Sds21}$ and any regulatory subunit (Extended Data Figure 2b,c), nor between $B56^{Par2}$ and $PP1^{Dis2}$ (Extended Data Figure 2d, 3). Leucine 482 of $B56^{Par2}$ occupies a position occupied by only valine or isoleucine in validated PP1 docking sites[12]. Changing this leucine to valine now allowed $PP1^{Dis2}$ to bind $B56^{Par2}$ (Extended Data Figure 2e).

Core K/RxVxF PP1 docking motifs can be accompanied by secondary motifs[12]. Although the $B55^{Pab1}$ docking site is an isolated K/RxVxF motif, the GLLR sequence of $B56^{Par1}$ bears a striking resemblance to the secondary element G/SILK/R[11,12] (Figure 2a green box). Mutating the GLLR motif ($B56^{par1}$*.G367V*) mimicked mutating the R/KxVxF motif ($B56^{par1}$*.K379AV381AF383A*) in abolishing interactions between $PP1^{Dis2}$ and $B56^{Par1}$ in two hybrid assays (Extended Data Figure 3), and compromising their ability to co-immunoprecipitate (Figure 2b, Extended Data Figure 2a). Mutating both motifs had an additive effect, severely compromising $B56^{Par1}$'s affinity for $PP1^{Dis2}$ in co-

immunoprecipitation assays (Figure 2b, Extended Data Figure 2a). Finally, the GLLR motif efficiently substituted for the characterised PP1-binding GILK motif of Cut12[20] (Extended Data Figure 4e-g). We conclude that GLLR is a “G/SILK/R” motif.

To confirm that the motifs we identified represent genuine PP1^{Dis2} docking sites, we generated PP1 docking site null mutants (PDSN) of B55^{Pab1} (*R52AV54AF56A*) and B56^{Par1} (*G367VK379AV381AF383A*) purified the respective holoenzymes and wild type controls from yeast cultures. The purified proteins were mixed with purified PP1^{Dis2} and the PP1^{Dis2} re-isolated to identify interacting partners. In each case, wild type but not PDSN holoenzymes were captured by PP1^{Dis2} (Extended Data Figure 5a-d). Moreover, PP1^{Dis2} co-migrated with the largest form of each of the wild type PP2A holoenzyme complexes in size-exclusion chromatography (Extended Data Figure 5e). We conclude that both B56^{Par1} and B55^{Pab1} contain genuine PP1^{Dis2} docking motifs.

To assess the mitotic defects of the *B55^{pab1}.PDSN* and *B56^{par1}.PDSN* PP1^{Dis2} docking site mutants (Figure 2c,d), we exploited transient arrest at the G2/M boundary with the temperature sensitive *Cdk1^{cdc2}.33* mutation to synchronise mitotic progression[21] (Figure 2e). Blocking PP1^{Dis2} recruitment to either B55^{Pab1} or B56^{Par1} in synchronised divisions generated significant errors in chromosome segregation and delayed the metaphase/anaphase transition (Figure 2e, Extended Data Figure 6a). To assay the timing of PP1^{Dis2} association with each PP2A holoenzyme we used a *Cdk1^{cdc2}.33* strain in which B55^{Pab1} and B56^{Par1} were fused to different epitope tags (*Cdk1^{cdc2}.33 B55^{pab1}.Pk B56^{par1}.HA*). PP1^{Dis2} levels in B55^{Pab1}. Pk precipitates peaked at metaphase (25-35 mins) whereas PP1^{Dis2} levels in B56^{Par1}. HA immunoprecipitates peaked later as spindles disassembled in telophase (60-70 mins) (Figure 2f).

An established PP2A-B56^{Par1} assay[22], in which PP1^{Dis2} displayed no activity (Extended Data Figure 6b-d), revealed a mitotic decline in bulk PP2A-B56^{Par1} activity before recovery at the start of the next cycle (Figure 3a). PP2A-B56^{Par1} activity was severely compromised when either the GLLR (GILK) or KEVLF (RxVxF) motifs were individually mutated (Extended Data Figure 6e,f) and abolished when both were simultaneously mutated to disrupt PP1^{Dis2} recruitment (Figure 3b; Extended Data Figure 6g). This indicated that PP1^{Dis2} could activate PP2A-B56^{Par1}; we confirmed this by adding immuno-purified PP1^{Dis2} to PP2A-B56^{Par1} that had been isolated by immunoprecipitation from synchronised cells that lacked PP1^{Dis2} (*PP1^{dis2}.*Δ) (Figure 3c). Moreover, PP1^{Dis2} activated wild type PP2A-B56^{Par1} but not the PP1 docking site mutant (Figure 3c,d, Extended Data Figure 6g, hi-iii), and genetically inhibited PP1^{Dis2}.T316D was unable to activate PP2A-B56^{Par1} (Figure 3c; Extended Data Figure 6h iv). Similar docking site dependent activity enhancement of purified PP2A-B56^{Par1} enzymes by purified PP1^{Dis2} (Extended Data Figure 5f) further confirmed that recruitment of active PP1^{Dis2} to the PP2A-B56^{Par1} docking site reactivated PP2A-B56^{Par1}.

Phosphorylation between the G/SILK/R and RxVxF motifs of a bipartite docking site can block PP1 recruitment[20]. Mass spectrometry analysis of B56^{Par1} from mitotic cells appeared to indicate phosphorylation on serine 378 between the GLLR and KEVLF motifs (boxed residue in Figure 2a; data not shown). Attempts to generate antibodies to recognise B56^{Par1}

when phosphorylated on S378 failed prompting us to generate a polyclonal antibody that would recognise B56^{Par1} when phosphorylated on both S377 and S378 (Extended Data Figure 7a). This antibody (B56-Phos) revealed increasing phosphorylation in mitosis that declined as PP1^{Dis2} was recruited to PP2A-B56^{Par1} (Figure 4a). Mutating S378 to alanine to block phosphorylation (*B56^{par1}.S378A*) promoted persistent PP1^{Dis2} recruitment to PP2A-B56^{Par1} and persistently high levels of PP2A-B56^{Par1} activity throughout mitosis that depended upon the presence of PP1^{Dis2} (Figure 3e,g,h; Extended Data Figure 6i,j). Conversely, when S378 was mutated to aspartic acid to mimic phosphorylation (*B56^{par1}.S378D*) this severely compromised PP1^{Dis2} recruitment and B56^{Par1}.S378D activity remained low throughout division (Figure 3f,i; Extended Data Figure 6k). Anaphase was delayed and frequently abnormal in *B56^{par1}.S378D* cells (Figures 3j), and it was striking that the persistent mitotic association of PP1^{Dis2} with PP2A-B56^{Par1} in *B56^{par1}.S378A* cells generated similar mitotic errors (Figure 3j). Thus, dynamic phosphate turnover on S378 appears to be crucial for orderly mitotic progression. As anticipated from the match to the consensus phosphorylation site for human Polo^{Plk1} (N/D/ExS/T)[23], Polo^{Plo1} was solely responsible for S378 phosphorylation (Figure 4b,c).

PP1^{Dis2} recruitment to B56^{Par1} at telophase (Figure 2f) indicated that serine 378 should be removed at this time, and the inability of *B55^{pab1}*.Δ cells to recruit PP1^{Dis2} to B56^{Par1} (Figure 4d) indicated that PP2A-B55^{Pab1} could be responsible for this dephosphorylation. In support of this, PP2A-B55^{Pab1} removed B56-Phos reactivity from B56^{Par1} in an *in vitro* assay (Extended Data Figure 7b). This phosphatase activity peaked during mitosis and was abolished when PP1^{Dis2} recruitment to B55^{Pab1} was blocked by removal of PP1^{Dis2}, when the PP1 docking site in B55^{Pab1} was ablated, and when genetically inhibited *PP1^{dis2}.T316D* was recruited (Figure 4f-i; Extended Data Figure 7c-f). Consistently, the failure of PP1^{Dis2} to associate with PP2A-B56^{Par1} in *B55^{pab1}*.Δ cells correlated with persistent phosphorylation on serine 378 throughout mitosis (*B55^{pab1}*.Δ; Figure 4e). Finally, purified PP1^{Dis2} enhanced the B56-Phos activity of purified PP2A-B55^{Pab1} in a docking site dependent manner (Extended Data Figure 5f).

In summary, PP1^{Dis2}, PP2A-B55^{Pab1} and PP2A-B56^{Par1} are linked in a phosphatase relay (Figure 4j, Extended Data Figure 8). At mitotic commitment all three activities are repressed[4] (Extended Data Figure 9a); subsequently PP1^{Dis2} activity recovers auto-catalytically as Cyclin B is degraded. The binding of repressed, T316 phosphorylated, PP1^{Dis2} to PP2A-B55^{Pab1} (Figure 2g) promotes rapid restoration of PP2A-B55^{Pab1} activity upon reduction of Cdk1-CyclinB activity. Reactivated PP2A-B55^{Pab1} can then begin to dephosphorylate S378 of B56^{Par1} but is antagonised by Polo^{Plo1}activity towards this site. Consequently, PP1^{Dis2} can only be recruited to PP2A-B56^{Par1} at telophase when Polo^{Plo1} declines (Figure 4j; Extended Data Figure 8). Thus, Cdk1-Cyclin B phosphorylation of PP1 at mitotic commitment[1,7-10] locks all three phosphatases in the “off” state. This lock is bolted through Cdk1-CyclinB phosphorylation-mediated reduction of PP1^{Dis2} levels. These controls join a range of other modes of PP1 and PP2A regulation, including Greatwall/ENSA control of PP2A-B55δ, and PP2A-B56 regulation by Bod1, to provide the accurate control of phosphorylation status that is critical for faithful cell division[1,6,11,24,25].

The conservation of the PP1 docking site motifs in PP2A regulatory subunits (Figure 2a) prompted us to assay association between human PP1 and PP2A enzymes. PP1α,β, and γ bound B56γ in yeast two hybrid assays, and PP1 co-immunopreciptiated with Flag epitope-tagged B56γ and B56δ expressed in mitotic human cells. Each of these interactions was abolished by mutation of the PP1 docking site motif (Figure 4k, Extended Data Figure 9b-d). Thus, the principle of a phosphatase relay whereby PP1 recruitment activates PP2A to control mitosis is conserved in human cells. It is notable that the NXS polo kinase consensus sequences in fungal B56s is replaced by SP and SQ motifs in metazoa (Figure 2A), suggesting that CDK/MAP kinases modulate PP1 docking to B56δ and B56γ while ATM/ATR/DNA-PK may co-ordinate docking to B56 α, β, ε. Furthermore these serine/threonine residues also conform to consensus motifs for AGC kinases including Aurora B (KXXS/T), while the threonine highlighted in yellow in Figure 2a could facilitate control by further kinases. We believe, therefore, that PP1 regulation of PP2A-B56 activity will emerge as a ubiquitous feature in diverse signalling contexts. While bulk biochemical assays reveal core principles of phosphatase control, local controls sit at the heart of many transitions[26]. Thus, we propose that competition between kinases and PP1 and PP2A holoenzymes at specific locations will generate locally active, dephosphorylated, phosphatases at times when assays show the activity of the bulk population is depressed.

Direct recruitment of PP1 to B55 and B56 subunits is unanticipated. Although the majority of predicted PP1 docking sites reside within regions that are predicted to be intrinsically disordered[11], PP1 recruitment to the docking sites of $B55^{Pab1}$, $B56^{Par1}$ and CenpE[11,27] suggest that this requirement is not axiomotic. A second conundrum is that the PP1 docking motifs are inaccessible in structures of the PP2A holoenzyme complexes solved so far[28-30]. PP1 docking site residues, and the equivalent residue to serine 378, form bonds that are crucial to the integrity of these structures, yet, contrary to predictions arising from these structures, mutation of these residues to alanine has no impact on the integrity of either PP2A-B55 or PP2A-B56 holoenzymes (Extended Data Figure 10). Moreover, Serine 378 is phosphorylated in purified PP2A-$B56^{Par1}$ complexes and holoenzymes isolated by one step immunoprecipitation (Extended Data Figure 5g 10c). Our data therefore add to established discrepancies between *in vivo* and *in vitro* PP2A-holoenzyme assembly[24] to suggest that alternative structures will emerge from structural studies of active enzymes that have undergone the extensive array of modifications required for activity that impact upon PP2A conformation *in vivo*[24].

Methods

Standard procedures[31,32] were used to grow and maintain yeast strains (Supplementary Table 1). Appropriately supplemented EMM2 synthetic medium was used throughout with the exception of TAP tag purification which used 10 × YES. The generation of size selected synchronous cultures was as described previously[33]. Two hybrid assays used the matchmaker gold system (Clontech 630489). “phospho-specific” rabbit poly-clonal antibodies were generated by Eurogentec. Commercial antibodies detected C^{Ppa1} and C^{Ppa2} (Cell Signaling, 2038), A^{Paa1} (Abcam, ab28350) and human B56ε (Santa Cruz sc-135223). In house poly-clonal antibodies detected $PP1^{Dis2}$ [20] and GFP. To detect associations between $PP1^{Dis2}$ and $B55^{Pab1}$ and $PP1^{Dis2}$ and $B56^{Par1}$ the complexes were isolated from

$2*10^8$ cells in the buffer (50 mM HEPES (pH 7.5), 50 mM NaF, 0.4 mM Na_3VO_4, 40 mM Na-β-glycerol phosphate, 1 mM EDTA, 50 mM NaCl, 0.1 % NP40, 1mM PMSF). The EnzChek (Molecular probes E12020) or histone H3 serine 10 dephosphorylation assays[34] monitored $PP1^{Dis2}$ activity (Extended Data Figure 1) with the use of recombinant Rabbit PP1γ (NEB P0754S), full length NIPP1 (Abcam, ab131705), Phos stop (Roche 04906845001) and potato acid phosphatase (Molecular probes E12020). Manufacturers instructions were followed for EnzChek assays (Molecular Probes E12020). For Histone H3 serine 10 assays, histone H3 (Millipore 14-4-11) that had been phosphorylated by established $Aurora^{Ark1}$ kinase assays[35] was used as a substrate. The dephosphorylation reaction was conducted in 20mM Hepes, 100mM NaCl, 1mM EDTA 0.1% NP40 at 30°C for 1 hour. An established $PP2A\text{-}B56^{Par1}$ activity assay employed $GST\text{-}Rec8^{391\text{-}561}$ phosphorylated by recombinant GST-Hhp2 (*S. pombe* casein kinase I) as a substrate[22]: $PP2A\text{-}B56^{Par1}$.HA was isolated from $2*10^8$ cells with 12CA5 antibody (Roche) under non-denaturing conditions. The dephosphorylation reaction was maintained at 30°C for 1 h, in; 50 mM Hepes (pH 7.5), 100 mM NaCl, 0.1% NP40, 2 mM $MnCl_2$, 2 mM DTT. ^{32}P levels in the substrate were determined with a Phosphoimager (BioRad). Phosphatase activity was calculated as the reduction of ^{32}P incorporation per unit $B56^{Par1}$ normalized to the activity of a standard sample from an asynchronous culture. $PP2A\text{-}B55^{Pab1}$ activity was monitored by detecting $B56^{Par1}$S377S378 phosphorylation with the phospho-specific antibody B56-Phos (Extended Data Figure 7a). $B56^{Par1}$.HA substrate from $6*10^8$ mitotically arrested cells[36] was independently isolated for three individual assays (scaling up substrate production failed due to substrate dephosphorylation and degradation during preparation). To isolate this $B56^{Par1}$·HA devoid of other subunits for $PP2A\text{-}B55^{Pab1}$ assays (Extended Figure 7b right panel) a TCA precipitation of total protein was re-suspended in a denaturing IP buffer (50 mM HEPES (pH 7.5), 50 mM NaF, 0.4 mM Na_3VO_4, 40 mM Na–β-glycerol phosphate, 1 mM EDTA, 200 mM NaCl, 0.2 % NP40, 1mM PMSF). The de-phosphorylation assay was performed at 30 °C for 1 h (100 mM Tris (pH 7.5), 150 mM NaCl, 10 mM DTT). PP2A and PP1 enzymes were purified by established sequential TAP and immuno-affinity/peptide elution methods[37]. For TAP tagging Econo-Pac Chromatography Column (Biorad 9704652) were packed with IgG Sepharose 6 FastFlow (GE Healthcare 170969-01) or Calmodulin Affinity Resin (Agilent technologies 214303-52). The following were used for subsequent affinity isolation; anti-HA Affinity Matrix (Roche 101677100), HA peptide (Sigma, I2149), Dynabeads A (Life Technologies) pre-loaded with $PP1^{Dis2}$ antibodies[20] according to manufacturers instructions and the SQNWHMTPPRKNK peptide for elution of $PP1^{Dis2}$ from the $PP1^{Dis2}$ polyclonal antibody. Coomassie (Brilliant Blue, Sigma, B2025-1EA) stained 4 – 12 % SDS NUPAGE gradient gels (Life Technologies, NP20327). Size-exclusion chromatography was performed on a Superdex 200 PC 3.2/30 column (VWR) using buffer B (50 mM Hepes pH 7.5, 100 mM NaCl, 0.1 % NP-40) collecting 50 µl fractions at a flow rate of 50 µl/ml[38]. All other *S. pombe* techniques were performed as described previously[20].

For immunoprecipitation of human complexes tetracycline-inducible HeLa cell lines were generated using a pcDNA5/FRT/TO vector (Invitrogen). Cells were grown in advanced DMEM (Invitrogen) supplemented with 2% fetal bovine serum and penicillin/streptavidin. Cells were blocked with thymidine (Sigma-Aldrich) for 24 hrs and released into fresh

medium with 300 nM nocodazole (Sigma-Aldrich) and 1 μg/ml tetracycline (EMD). Prometaphase cells were collected by mitotic shake-off after 12 hrs. Cells were lysed for 20 minutes on ice in extraction buffer A (50 mM Tris-HCl pH=8.0, 150 mM NaCl, 0.2 % NP-40, 1 mM EDTA, complete inhibitor cocktail tablet (Roche), 0.2 μM microcystin (LGC-Promotech)) and lysates cleared by centrifugation for for 15 min 12,000 *g* at 4 °C. Protein complexes were precipitated for 1,5 hrs at 4°C with anti-FLAG (M2; Sigma-Aldrich) covalently coupled to Dynabeads (Invitrogen), washed in extraction buffer, and bound proteins eluted with LDS-sample buffer (Invitrogen) before analysis by immunoblotting[38]. Anti-Flag and anti-PP1 (E-9; Santa Cruz sc-7482) were used at 1;1,000.

Extended Data

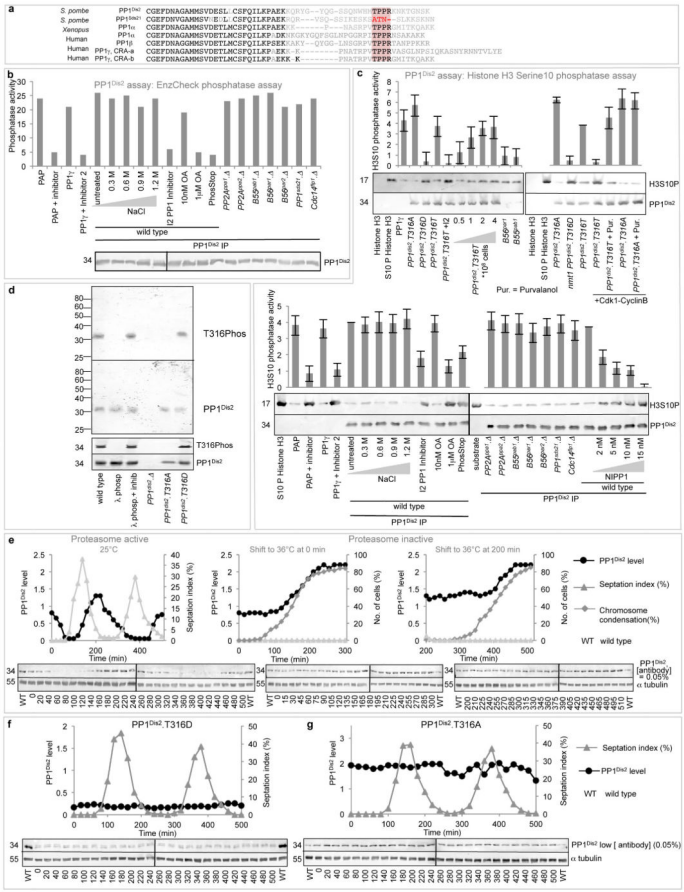

Extended Data Figure 1. PP1 phosphorylation by Cdk1-Cyclin B on T316 represses activity and reduces abundance in a manner that is mimicked by mutation of the target site to an acidic residue in PP1^{Dis2}.T316D

a) Clustal W alignments of the carboxyl terminal residues of the indicated PP1 isoforms. The Cdk1-Cyclin B phosphorylation site is highlighted by red shading. Red letters within this region of shading highlight the clear deviation from this consensus in the *S. pombe* PP1^{Sds21} isoform. PP1^{Sds21} is unable to bind to either B55^{Pab1} or B56^{Par1}. The molecular basis for this inability of PP1^{Sds21} to bind the regulatory subunits of PP2A remains to be established. The initial threonine in the *S. pombe* PP1^{Dis2} shaded consensus sequence region

is T316. b,c) Phosphatase assays of the indicated samples with activity detection by either EnzChek (b) or histone H3 serine 10 dephosphorylation (c – a second established PP1 activity assay[34]). For each assay the graphs show arbitrary units. Bars=standard deviation. Identical results were obtained with each assay. The similarity between the recombinant Rabbit PP1γ and potato acid phosphatase (PAP) activities indicate that both reactions measure PP1 activity. The inhibition of the activity of $PP1^{Dis2}$ precipitates by 1 μM, but not 10nM Okadaic acid (OA) and suggest that it is the $PP1^{Dis2}$ activity rather than any coprecipitating PP2A activity that is being monitored in these assays. This view is consolidated by the inhibition of activity in both assays by the PP1 specific inhibitor NIPP1 (2, 5, 10 and 15 nM; panel c and Figure 1a). 5nM is routinely used to inhibit mammalian PP1[34,39]. Manufacturers instructions were followed for EnzChek assays. For Histone H3 serine 10 assays, histone H3 that had been phosphorylated by $Aurora^{Ark1}$ kinase[35] was used as a substrate. The dephosphorylation reaction was conducted in 20mM Hepes, 100mM NaCl, 1mM EDTA 0.1% NP40 at 30 °C for 1 hour. The molarity of NaCl indicates the salt concentration of the buffer used for the immunoprecipitation, not the molarity within the phosphatase reaction. All phosphatase reactions for each substrate were conducted under identical conditions. A 1.2M NaCl, buffer was used to isolate the $PP1^{Dis2}$ for the experiments in Figures 3c,d and Extended Data Figure 6d, giii, hii-iv. The level of PP1 activity detected in either assay shown in panel b and panel c was the same irrespective of the NaCl concentration in the buffer used to isolate the $PP1^{Dis2}$. Phos stop is a universal phosphatase inhibitor. The key conclusion from all these assays is that the $PP1^{Dis2}$.T316D protein has a similar level of activity as the Cdk1-Cyclin B phosphorylated enzyme and so behaves as a “genetically inhibited” phosphatase in the subsequent experiments described in the manuscript. d) Validation of the T316Phos antibody. $PP1^{Dis2}$ immunoprecipitates from the indicated strains were treated as indicated and probed with either $PP1^{Dis2}$ or T316Phos polyclonal antibodies. e-g) Cultures synchronised with respect to cell cycle progression by size selection through elutrient centrifugation probed with the $PP1^{Dis2}$ antibodies at the high dilution that revealed the fluctuations in $PP1^{Dis2}$ levels in Figure 1c. Graphs show the septation index alongside the $PP1^{Dis2}$ levels in each sample normalised to the level of the α-tubulin loading control and a sample from an asynchronous culture that was run on each gel. e) Samples from this $Rpn12^{mts3.1}$ culture was split into three immediately after elution and one third was maintained at the permissive temperature of 25°C for the remainder of the experiment, another third was immediately shifted to 36°C to inactivate this essential component of the proteasome 26S subunit[40], while the inactivating temperature shift of the remaining third was done 200 minutes later, after cells had completed one round of division at 25 °C. Note that the mitotic decline in $PP1^{Dis2}$ levels at the permissive temperature as cells progress from mitotic commitment to the metaphase anaphase transition is not seen at 36 °C when the proteasome function is inactivated, despite the fact that the chromosome condensation index indicates that over 60% of cells have arrested cell cycle progression with a metaphase spindle. f,g) $PP1^{Dis2}$ levels fail to oscillate when the Cdk1-Cyclin B phosphorylation site at position T316 is mutated. A switch to the phosphomimetic glutamic acid results in persistently low protein levels (f) while levels are persistently high upon mutation to alanine to block phosphorylation (g). Because these levels remain constant through the cell cycle these normalised levels have been superimposed upon the data from a wild type culture in Figure 1c to show each level relative to the oscillating wild type protein

levels. The septation profile in Figure 1c is the profile for that wild type culture. The septation profile in Figure 1c does not contain any data from either of the cultures shown here in Extended Data Figures 1f, g. The septation profiles for each mutant culture are shown here in panels f and g.

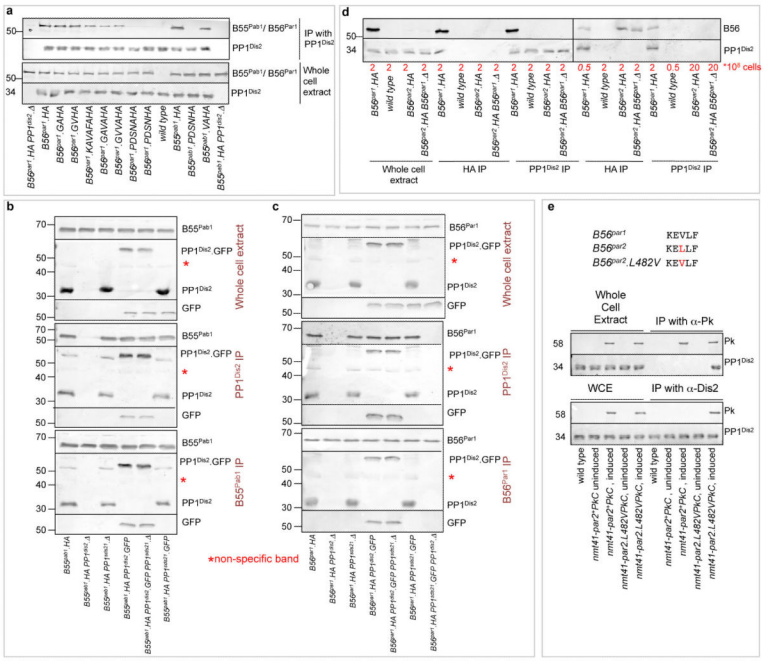

Extended Data Figure 2. Association of PP1^{Dis2} with the PP2A regulatory subunits B56^{Par1} and B55^{Pab1}

a-d) Immunoprecipitation reactions in which PP1^{Dis2} polyclonal antibodies precipitated and detected PP1^{Dis2}, GFP antibodies precipitated and detected either PP1^{Dis2} or PP1^{Sds21} functional fusion proteins[19] or 12CA5 monoclonal antibodies precipitated HA tagged B55^{Pab1} and B56^{Par1} regulatory subunits of the PP2A phosphatase, as indicated. These blots establish that the association between PP1^{Dis2} and both B56^{Par1} and B55^{Pab1} was independent of PP1^{Sds21} function. No association was detected between PP1^{Sds21} and any PP2A regulatory subunit (including B56^{Par2} (data not shown)). In b and c the red asterisk indicates a non-specific band that is detected by the anti-GFP antibodies. d) No association was detected between B56^{Par2} and PP1^{Dis2}, even when cell numbers in the precipitates were increased 10 fold (numbers shown in red under the panel are X × 10^8 cells per ml) to enhance the sensitivity of detection and the *B56^{par1+}* gene encoding the B56^{Par1} subunit was deleted in an attempt to remove any competition from this primary B56 isoform. e) Expression of *B56^{par2}.PkC* and *B56^{par2}. L482VPkC* genes from the pINT41PkC integration vector[32] was derepressed by removal of thiamine. B56^{Par2} proteins (upper) or PP1^{Dis2} (lower) were precipitated with antibodies against the Pk epitope (upper) or PP1^{Dis2} peptide (lower) respectively and these immunoprecipitation reactions were run alongside aliquots of the equivalent whole cell extracts (WCE), before western blotting detected PP1^{Dis2} and B56^{Par2} fusion proteins. In both assays, the PP1 docking site mutant in which the leucine of B56^{Par2} was replaced with the valine of B56^{Par1} (B56^{Par2}.L482V) associated with PP1 whereas the wild type B56^{Par2} protein did not.

Europe PMC Funders Author Manuscripts

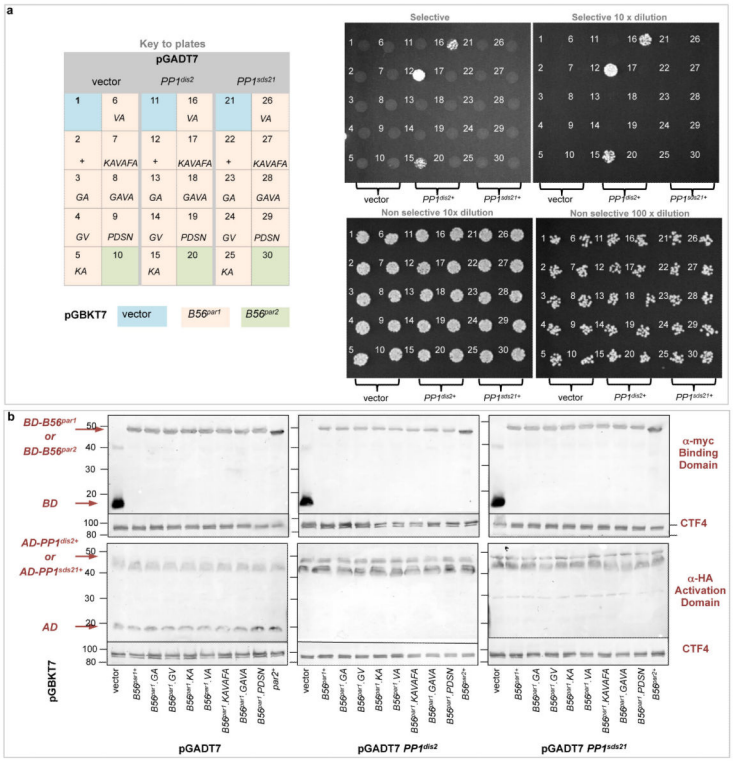

Extended Data Figure 3. Yeast two hybrid assays reveal docking site dependent association between B56^{Par1} and PP1^{Dis2}

Yeast two hybrid assays in which *PP1^{dis2+}* and *PP1^{sds21+}* sequences were fused to the activating domain of Gal4 and the indicated version of the core homology domains of the PP2A regulatory subunits *B56^{par1+}* (encoding amino acids 112-424) and *B56^{par2+}* (encoding amino acids 213-525) were fused to the Gal4-DNA binding domain according to the procedures of the matchmaker gold yeast two hybrid system. b) Blotting the cell extracts with 12CA5 and 9E10 monoclonal antibodies that recognized HA and myc epitopes within the cassettes harbouring the activation (HA) and DNA binding domains (myc) indicated that equivalent protein expression levels were achieved for each version of the protein. Probing for the DNA replication factor Ctf4 was used as a loading control[41]. Thus, the failure of the PP1 docking site mutants to interact with *PP1^{dis2+}* suggests that the change in the PP1 docking site abolished the affinity between the two molecules.

Europe PMC Funders Author Manuscripts

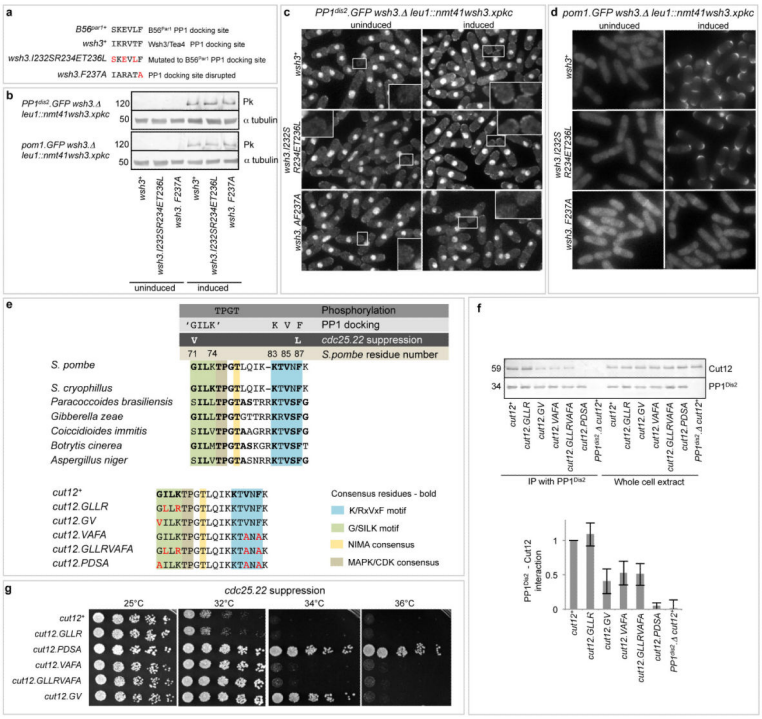

Extended Data Figure 4. Validation of the SKEVLF and GLLR motifs of the PP1 docking consensus site of B56^{Par1} in the polarity protein Wsh3/Tea4 and the mitotic regulator Cut12

The morphology protein Wsh3/Tea4 is required to recruit PP1^{Dis2} to cell tips[19]. Wsh3/Tea4 recruited PP1 promotes the de-phosphorylation of the DYRK family kinase Pom1[42]. De-phosphorylation of Pom1 promotes its association with the cell cortex. Subsequent auto-phosphorylation diminishes this new-found affinity for the cortex until the kinase looses its affinity for the cortex. Because Wsh3/Tea4 is only found at cell tips, Pom1 only associates with the cortex at the tips[42]. We exploited this relationship to test the ability of the SKEVLF sequence in the PP1 docking consensus site of B56^{Par1} to function as a PP1^{Dis2} docking site *in vivo*. a) The indicated *wsh3* alleles were cloned into the pINTL41PkN vector[32] and integrated at the *leu1* locus before introduction into *wsh3*.Δ background in which the endogenous *wsh3*$^{+}$/*tea4*$^{+}$ gene had been deleted. b) Expression of the transgenes was repressed by the addition of thiamine to culture medium (uninduced) before filtration into thiamine free medium induced expression of each allele 24 hours later (induced). c) PP1^{Dis2}.GFP was not enriched at cell tips in the absence of *wsh3* induction. Induction of the wild type or *wsh3.I232SR234ET236L* allele in which the SKEVLF motif of the B56^{Par1} PP1^{Dis2} docking site was substituted for the native IFRVTF motif of Wsh3/Tea4 led to the recruitment of PP1^{Dis2}.GFP to cell tips whereas expression of the PP1 docking site mutant *wsh3. F237A* failed to do so. d) Pom1 recruitment to cell tips upon expression of both the wild type and SKEVLF alleles, but not the PP1 docking site alleles indicated that the PP1^{Dis2} recruited to Wsh3/Tea4 by the SKEVLF allele was functionally indistinguishable from that recruited by the wild type molecule. e-g) Commitment to mitosis is promoted by the activation of Cdk1-CyclinB. Cdk1-CyclinB activity is regulated by the level of phosphorylation on threonine 14 and tyrosine 15 within its ATP binding site. Wee1 kinase phosphorylates these residues while Cdc25 removes the phosphate to trigger mitotic

Europe PMC Funders Author Manuscripts

commitment[43]. The lack of Cdc25 phosphatase activity achieved by incubating cells harbouring the temperature sensitive *cdc25.22* mutation at temperatures above 34 °C kills cells because they are unable to remove the inhibitory phosphate from Cdk1. The *cut12.s11* and *cut12.s14* mutations enable *cdc25.22* cells to divide at 34°C [20,44]. *cut12.s11* is a G71V mutation at the start of a highly conserved bipartite PP1 docking site **GILK**$_{\text{TPGTLQIK}}$**KTVNF**. *cut12.s14* is a F87L mutation at the end of the same docking motif[20]. (e) Alignment of the conserved PP1 docking site of Cut12 homologues from the indicated fungi and the mutations generated in each of the indicated *cut12* alleles. Mutation of the PP1 docking site of *S. pombe* Cut12 to abolish the function of either the GILK or the KxVxF motifs of Cut12 reduces PP1^{Dis2} association in immunoprecipitation assays (f) and suppresses the lethal mitotic commitment defect of *cdc25.22* (g). Simultaneous mutation of both motifs abolishes PP1 association in immunoprecipitation assays and confers a higher level of suppression of *cdc25.22* (g) that can enable cells to survive complete removal of *cdc25*$^{+}$ coding sequences[20]. We asked whether the GLLR sequence found upstream of the B56^{Par1} KxVxF motif (Figure 2a) would substitute for the GILK sequence of Cut12 in both the co-immunoprecipitation and *cdc25.22* suppression assays. In both cases it could. The association between PP1^{Dis2} and Cut12 in the *cut12.I72LK74R* mutant that converts the GILK motif to a GLLR was indistinguishable from wild type. Also, the G71V mutation of *cut12.s11* suppressed *cdc25.22* whereas *cut12.I72LK74R* did not (g). Thus, the function bestowed on Cut12 by the GILK sequence is fully maintained upon substitution with GLLR indicating that GLLR is a functional variant of GILK. f) bars = standard deviation.

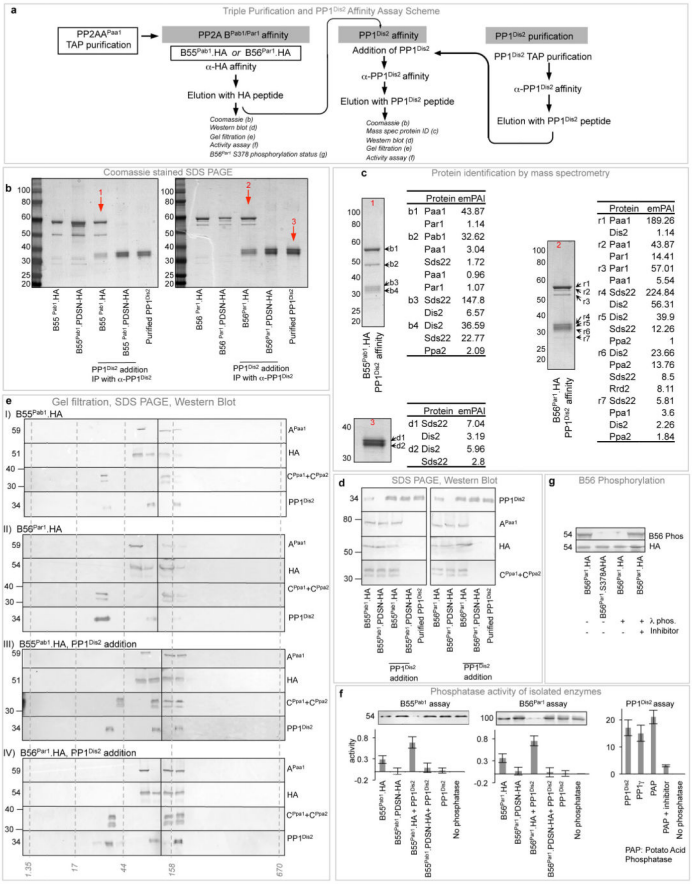

Extended Data Figure 5. *in vitro* association of purified PP1^{Dis2} with PP2A-B55^{Pab1} and PP2A-B56^{Par1} complexes in a docking site dependent manner

The tandem affinity purification steps employed in Extended Data Figure 10e were followed by immuno-affinity with antibodies directed either against the HA epitope on B55^{Pab1}.HA or B56^{Par1}.HA fusion proteins or the unique sequence SQNWHMTPPRKNK in the C terminus of PP1^{Dis220} using anti-HA Affinity Matrix followed by elution with HA peptide, or Dynabeads A pre-loaded with PP1^{Dis2} antibodies[20] followed by elution with the SQNWHMTPPRKNK peptide respectively. b) Coomassie stained 4 – 12 % SDS NUPAGE gradient gels. In each case the first two sample lanes show the purified wild type and PDSN PP2A holoenzymes and the fifth lane shows the purified PP1^{Dis2} enzyme. This quantity of PP1^{Dis2} was mixed with the quantity of each PP2A complex shown in lanes 1 and 2 before re-isolated of PP1^{Dis2} via affinity for beads bearing PP1^{Dis2} antibodies. This PP1^{Dis2} (and any associated partner molecules) was then eluted from these beads with the SQNWHMTPPRKNK peptide and the eluted proteins run in lanes 3 and 4 of each gel. For both the B55^{Pab1} (left) and B56^{Par1} (right) PP2A holoenzymes the wild type but not the PDSN complex bound to PP1^{Dis2}. The numbered arrows indicate the lanes from which bands were excised for protein identification by mass spectrometry in panel c. c) Protein identification by mass spectrometry of the indicated bands from the lanes on the SDS PAGE gels highlighted by the numbered arrows in panel b. emPAI scores[45] show that the purified PP1^{Dis2} preparations used for the *in vitro* reconstitution reaction and run in lanes 5 of the two gels in panel b also contained the conserved and well characterised PP1 partner

Europe PMC Funders Author Manuscripts

Sds22[46,47]. emPAI scores for the bands found in the reconstituted PP2A holoenzyme/PP1 complexes show that the predominant molecule identified in each complexes corresponds with a known subunit of the PP2A complex, PP1^{Dis2} or Sds22. d) Western blotting to detect the indicated components in the complexes used for panels b and c. The epitope tagged regulatory B55^{Pab1} and B56^{Par1} molecules were detected with antibodies against the HA tag, while the catalytic C^{Ppa1} and C^{Ppa2} and scaffolding A^{Paa1} subunits of PP2A were detected with commercial antibodies. e) Western blots of gel filtration chromatography fractions of either the isolated PP2A holo-enzyme complexes (i, ii) or the eluted PP2A holoenzyme/PP1 quaternary complexes (iii, iv) corresponding to lanes 1 and 3 of the two SDS NUPAGE gels of panel b. Note the very low level of PP2A-B55^{Pab1}/PP1^{Dis2} and PP2A-B56^{Par1}/PP1^{Dis2} quaternary complexes in the isolated PP2A holoenzyme preparations in panels i and ii. Migration of the different complexes at the appropriate size suggests that the procedures used isolated correctly folded proteins. f) Phosphatase assays of the isolated enzymes used in panels b-e show that these molecules are active phosphatases and so the procedures used isolated functional, correctly folded complexes rather than denatured, inappropriately folded, proteins. For each assay n = 5. bars = standard deviation. g) B56-Phos blots of the TAP and HA purified holoenzyme complex preparations used in panel c alongside a similarly purified PP2A-B56^{Par1}.S378A holoenzyme complex.

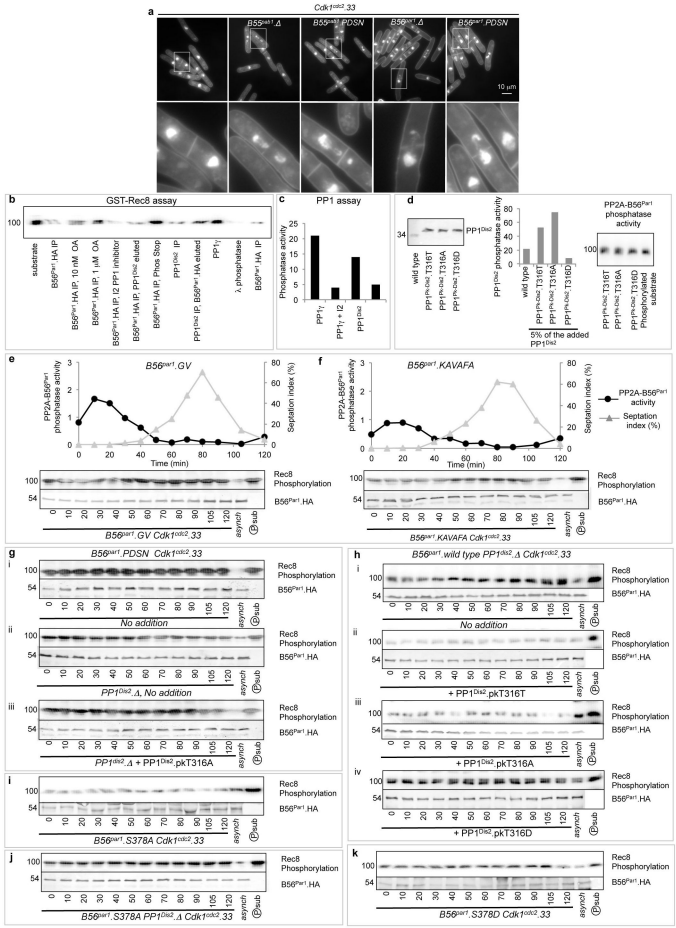

Europe PMC Funders Author Manuscripts

Extended Data Figure 6. Mitotic enhancement of PP2A-B56^{Par1} activity relies upon recruitment of active PP1^{Dis2} and is required for accurate chromosome segregation

a) DAPI staining of the *Cdk1^{cdc2}.33* strains in which mitotic progression has been synchronised by transient arrest at the restrictive temperature of 36°C. While two evenly sized chromatin masses are generated by the anaphase in wild type cells, chromosome segregation is uneven in the mutant lines and lagging chromosomes are frequently observed. The frequency of phenotypes is presented in Figure 2e. b) The PP2A-B56^{Par1} phosphatase assay of Ishiguro et al. in which recombinant GST-Rec8$^{391\text{-}561}$ was phosphorylated by a fusion between glutathione and *S. pombe* casein kinase I (Hhp2) that had also been produced in *E. coli*[22]. PP2A-B56^{Par1}.HA was isolated from 2*10^8 cells with 12CA5 antibody under non-denaturing conditions. Phosphatase activity was calculated from the reduction of ^{32}P incorporation in the GST-Rec8$^{391\text{-}561}$ substrate per unit B56^{Par1}.HA. The level obtained in this assay (and every assay presented in this study) was normalized to the reduction in substrate phosphorylation displayed by a B56^{Par1} precipitate from 2 × 10^8 cells of an asynchronous *B56^{par1}.HA* culture run on the same gel (the second lane in panel b)). OA = Okadaic acid. c) PP1^{Dis2} activity assays conducted in parallel with the same samples used in panel b. These assays established that both the recombinant Rabbit PP1γ and the PP1^{Dis2} samples that were added to the PP2A-B56^{Par1} assay in panel a both contained PP1 phosphatase activity. We conclude that we have successfully re-established the phosphatase assays described by Ishiguro *et al*[32] and that the addition of PP1 to this assay did not alter the phosphorylation status of the phosphorylated GST-Rec8 substrate indicating that PP1^{Dis2} displays no activity towards phosphorylated GST-Rec8 used in this PP2A-B56^{Par1} enzyme assay. d) This panel presents blots of protein levels (left) PP1^{Dis2} activity assays (centre) and PP2A-B56^{Par1} phosphatase assays (right) of the PP1^{Dis2} samples used in the add back experiments in panels giii and hii-iv. The blot of PP1^{Dis2} levels on the left shows that similar levels of the different PP1^{Dis2} proteins were added in each case, while the central panel shows that these samples possessed PP1^{Dis2} activity. The panel on the right shows that none of the PP1^{Dis2} samples exhibited any activity in the PP2A-B56^{Par1} phosphatase assay. In other words, there was no PP2A-B56^{Par1} in these pull downs despite the fact that PP1^{Dis2} is able to bind to PP2A-B56^{Par1}. This absence of PP2A-56^{Par1} from these samples is either due to the fact that only a minor fraction of the PP1^{Dis2} complex formed a complex with PP2A-B56^{Par1}, or, as we anticipate, that the high salt (1.2M NaCl) conditions we used in the immunopreciptation reactions that isolated these PP1^{Dis2} molecules for the “add back” experiments (panels g,h and Figure 3c,d) had disassociated any PP2A-B56^{Par1} molecules that partnered these PP1^{Dis2} molecules *in vivo*.

e-k) PP2A-B56^{Par1} assays as for panel b. A quantitative plot of the data in panel gi is shown in main Figure 3b while the data from giii and hi-hiv are represented in the plots in Figure 3c and d while data from i-k are shown in Figure 3g-i. For the experiments in panels g ii iii and h we exploit the redundancy between PP1^{Dis2} and PP1^{Sds21} to use PP1^{Sds21} to provide essential PP1 function and support the viability of *PP1^{dis2}.*Δ cells[2]. The PP2A-B56^{Par1} complexes isolated from these cells have therefore never been exposed to PP1^{Dis2} regulation and so will be fully phosphorylated on PP1^{Dis2} target sites. The addition of PP1^{Dis2} *in vitro* enabled us to assesses the impact of dephosphorylation of these sites. To ensure that there could be no cell cycle dependency to any outcome in these assays we assessed the impact of PP1^{Dis2} addition on PP2A-B56^{Par1} samples from all stages of a *Cdk1^{cdc2}.33* synchronised

Europe PMC Funders Author Manuscripts

mitosis. The data from these experiments that is presented in Figure 3 and this figure panels d, g and h clearly demonstrate that the addition of active $PP1^{Dis2}$ to naïve PP2A-$B56^{Par1}$ complexes that have never been exposed to $PP1^{Dis2}$ *in vivo* was able to reactivate the PP2A activity as long as the $PP1^{Dis2}$ docking site within $B56^{Par1}$ was intact. In contrast $PP1^{Dis2}$ addition failed to reactivate these naïve PP2A-$B56^{Par1}$ complexes when the $PP1^{Dis2}$ docking site in $B56^{Par1}$ had been mutated to block $PP1^{Dis2}$ recruitment, or the Cdk1-CyclinB inhibition site at T316 of $PP1^{Dis2}$ had been mutated to aspartic acid to mimic the phosphorylated state.

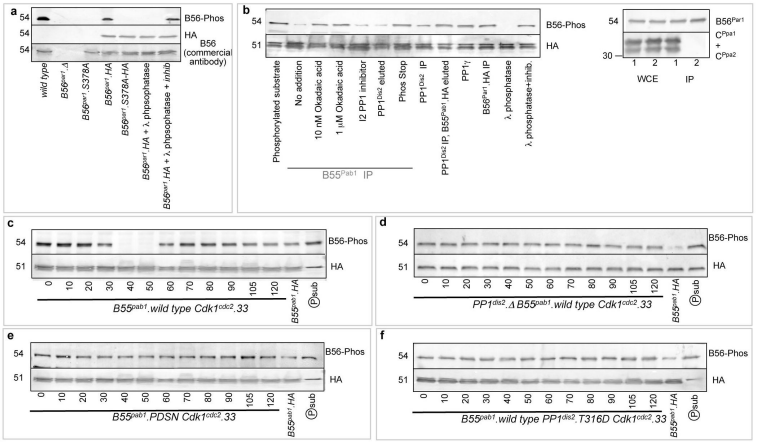

Extended Data Figure 7. Residue 378 within the PP1 docking site of $B56^{Par1}$ was dephosphorylated by PP2A-$B55^{Pab1}$ that had been activated by $PP1^{Dis2}$ recruitment to its own PP1 docking site

a) Validation of the B56-Phos antibody that was raised against and affinity purified with a peptide in which residues corresponding to the serines at 377 and 378 were each phosphorylated. Immunoprecipitates in which the 12CA5 monoclonal antibody was used to recognise the HA epitope on a $B56^{Par1}$.HA fusion protein or commercial rabbit antibodies raised against human B56ε were used to precipitate $B56^{Par1}$ and probed as indicated. b) Validation of the PP2A-$B55^{Pab1}$ activity assay. This assay exploits the fact that PP2A-$B55^{Pab1}$ removes B56-Phos reactivity from $B56^{Par1}$.HA. The phosphorylated $B56^{Par1}$.HA substrate was precipitated from cells in which mitotic progression had been arrested by incubation of *$Eg5^{cut7}$.24* cells at the restrictive temperature for 3 hours. *$Eg5^{cut7}$.24* is a temperature sensitive mutation in the kinesin 5 motor protein that is required for inter-digitation of the two halves of the bipolar spindle[36]. To ensure that these $B56^{Par1}$ precipitates were free of any $B56^{Par1}$ partners, the total protein content of intact cells was precipitated by TCA treatment before cells were homogenised and re-suspended in, 2% SDS. After a centrifugation clearing step, the addition of 1% Triton ×100 to the resultant supernatant sequestered the SDS into micelles thereby generating conditions for immuno-precipitation (IP) of phosphorylated $B56^{Par1}$.HA substrate. Lane 2 in the right hand panel shows that that this procedure disassociated the $B56^{Par1}$ subunit from the other subunits of the tri-partite PP2A-B56 complex whereas non-denaturing IP conditions (lane 1) do not. The C^{Ppa1} and C^{Ppa2} catalytic subunits are detected with a commercial antibody. The $B56^{Par1}$ samples generated in this way were incubated with the indicated components. “eluted” indicates reactions in which the $B55^{Pab1}$ immunoprecipitate was incubated with a peptide

corresponding to the PP1^{Dis2} docking site on B56^{Par1} (CWPKVNSSKEVLF) to disassociate the PP1^{Dis2} enzyme from the PP2A-B55^{Pab1} complex before a re-purification isolated the PP1^{Dis2} complex once more. It was this re-isolated PP1^{Dis2} that was used for the assay in lane 9 while the residual PP2A-B55^{Pab1} was used in the assay in lane 6. The impact of this disassociation can be seen by comparing lanes 8 and 9. The PP1^{Dis2} immunoprecipitate exhibited a low level of B56-Phos phosphatase activity when the elution step was not performed. Displacement of partner molecules through peptide incubation removed the activity that reduced B56-Phos reactivity in the un-eluted PP1^{Dis2} precipitates. The inhibitor profiles, all support the conclusion that this assay specifically detected PP2A-B55^{Pab1} activity. Phos-Stop is a commercial pan-phosphatase inhibitor. c-f) PP2A-B55^{Pab1} activity assays of cultures in which mitotic progression had been synchronised by the *Cdk1^{cdc2}.33* arrest/release protocol. The quantification of these assays is presented in Figure 4f-i.

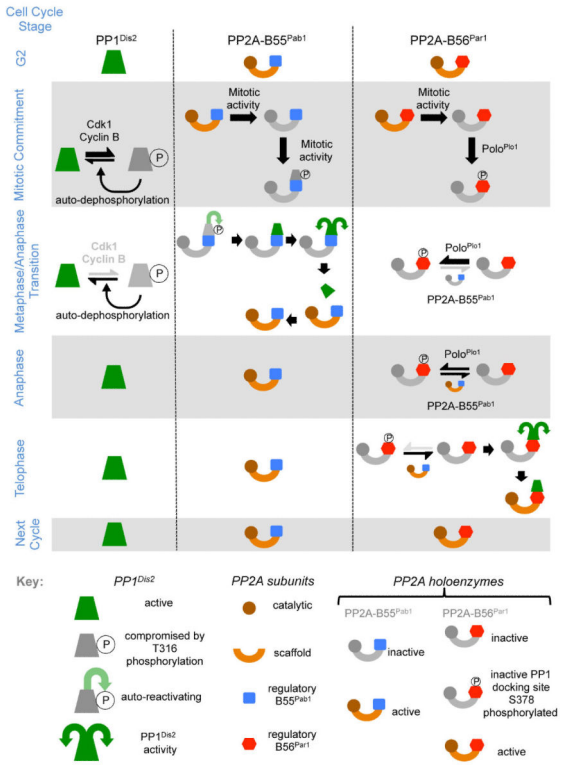

Extended Data Figure 8. Mitotic control of phosphatase activities

A schematic representation of the control and activity levels of the three phosphatase activities. This view is derived from bulk activity assays. We believe that localised reactions at particular times at discrete locations will differ, however the basic relationships between the three phosphatases outlined here will apply.

Left) As previously established in a number of studies[1,7-10] PP1^{Dis2} activity is repressed by Cdk1-Cyclin B phosphorylation upon mitotic commitment through phosphorylation on T316 at a rate that exceeds the rate at which auto-dephosphorylation re-activates inhibited PP1. PP1^{Dis2}T316 phosphorylation also targets PP1^{Dis2} for destruction to further reduce PP1^{Dis2} activity although the majority of the protein persists. It is currently unclear whether this reflects a highly localised destruction of a particular pool of PP1^{Dis2} in its entirety or a rate

of destruction across the population that is simply too slow to out compete with synthesis. Cyclin B destruction curtails the inhibitory phosphorylation on T316 enabling $PP1^{Dis2}$ to auto-reactivate and persist in an active state for the remainder of mitosis.

Middle) $PP2A\text{-}B55^{Pab1}$ activity is inhibited upon mitotic commitment (Extended Data Figure 9a). The mechanism by which this inhibition is achieved is currently unclear. The inactivated $PP2A\text{-}B55^{Pab1}$ recruits T316 phosphorylated (and therefore catalytically compromised) $PP1^{Dis2}$ upon mitotic commitment. Cyclin B destruction upon the metaphase anaphase transition promotes $PP1^{Dis2}$ reactivation (lefthand panel). The reactivation of the $PP2A\text{-}B55^{Pab1}$ associated $PP1^{Dis2}$ enables this $PP1^{Dis2}$ to reactivate $PP2A\text{-}B55^{Pab1}$. $PP1^{Dis2}$ then disassociates from $B55^{Pab1}$. The molecular basis for the staged association between $PP1^{Dis2}$ and $B55^{Pab1}$ upon mitotic commitment and dissociation at the metaphase anaphase transition remains to be established. $PP2A\text{-}B55^{Pab1}$ persists in an active state for the remainder of mitosis.

Right) $PP2A\text{-}B56^{Par1}$ activity is inhibited upon mitotic commitment (Extended Data Figure 9a). The mechanism by which this inhibition is achieved is currently unclear. $Polo^{Plo1}$ activation upon mitotic commitment enables it to phosphorylate serine 378 within the PP1 docking site on $B56^{Par1}$ to block $PP1^{Dis2}$ recruitment to this B' regulatory subunit of the PP2A-B56 holoenzyme. This phosphorylation persists to block $PP1^{Dis2}$ recruitment until telophase when the balance between $Polo^{Plo1}$ kinase and $PP2A\text{-}B55^{Pab1}$ phosphatase activities tips in favour of $PP2A\text{-}B55^{Pab1}$ to remove phosphate from serine 378, thereby promoting the recruitment of active, T316 dephosphorylated $PP1^{Dis2}$. $PP1^{Dis2}$ recruitment enables this phosphatase to reactivate the $PP2A\text{-}B56^{Par1}$ holoenzyme.

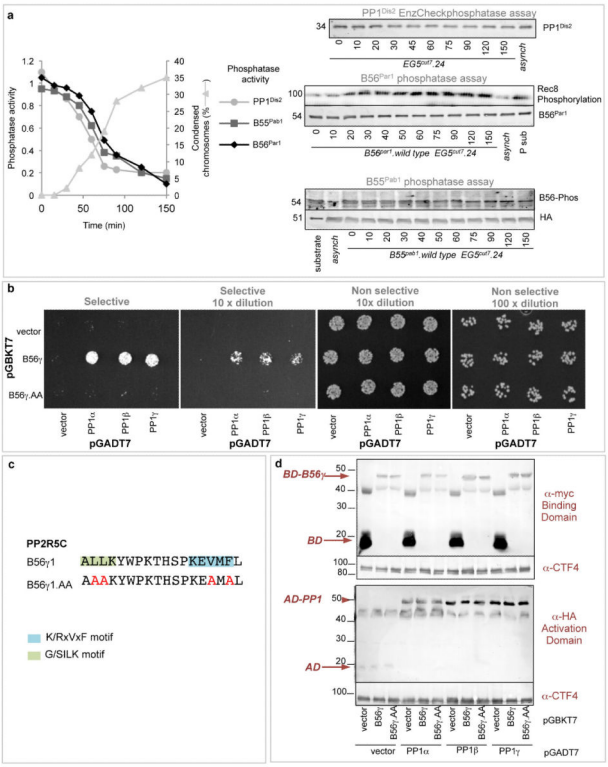

Extended Data Figure 9. PP1^{Dis2}, PP2A-B55^{Pab1} and PP2A-B56^{Par1} activities decline as cells arrest cell cycle progression in mitosis and association between human PP1 and PP2A B56 isoforms

a) The temperature of *Eg5^{cut7}.24 B55^{Pab1}.HA, Eg5^{cut7}.24 B55^{Par1}.HA* and *Eg5^{cut7}.24* cultures that had been grown overnight to early-log phase in supplemented EMM2 medium at 25°C was increased to 36°C at t=0 to inactivate this kinesin 5 and so arrest cell cycle progression in mitosis[36]. Samples were taken for the phosphatase assays and to monitor the degree of mitotic arrest by scoring the frequency of cells with condensed chromosomes[36]. Protein phosphatase assays were conducted as described for Extended Data Figures 1b, 6b and 7b. Each activity declined as the frequency of cells in which the inability to form a bipolar spindle has triggered a mitotic arrest due to activation of the spindle assembly checkpoint. b) Two hybrid assays with the indicated human PP1 isoforms with wild type and mutant isoforms of the conserved core domain (sequences encoding amino acids 84-400) of human B56δ. c) The mutations introduced in each case. d) Blotting the cell extracts from the two hybrid clones shown in panel e with 12CA5 and 9E10 monoclonal antibodies that recognized HA and myc epitopes within the cassettes harbouring the Gal4 activation and DNA binding domains respectively indicated that equivalent protein expression levels were achieved for each version of the protein. Thus, the failure of the PP1 docking site mutants indicates that the change in the PP1 docking site abolished the affinity between the two molecules.

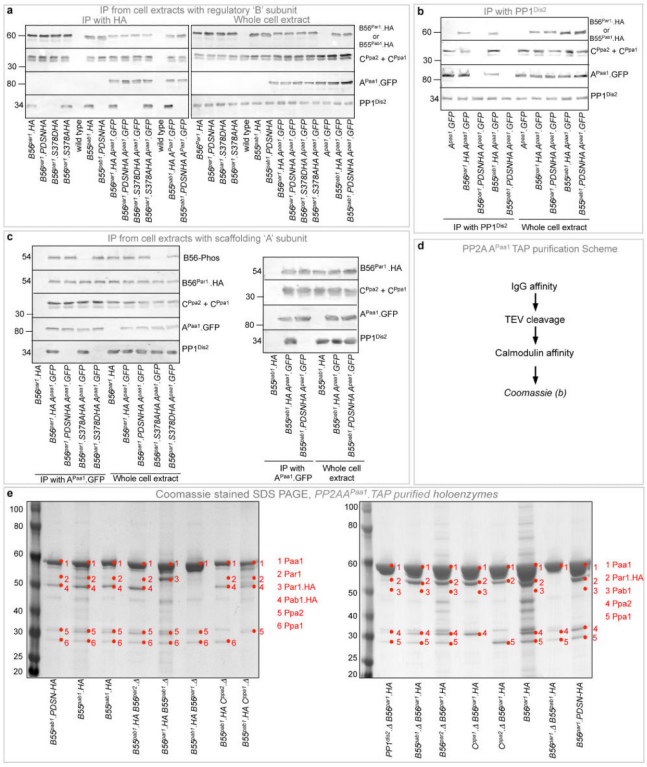

Extended Data Figure 10. PP1 docking site mutations do not alter the stoichiometry of PP2A subunits in immunoprecipitation assays or of holoenzymes isolated by TAP tag purification

a-c) Immunoprecipitation reactions from cell extracts of the indicated strains in which the 12CA5 antibodies were used to precipitate epitope tagged versions of the B55^{Pab1} or

B56^{Par1} PP2A regulatory subunits or poly-clonal anti-GFP antibodies were used to precipitate a GFP tagged version of the A^{Paa1} PP2A scaffolding subunit. Although mutation of either the PP1 docking site motif sequences or the *B56^{par1}.S378D* mutation abolished PP1 precipitation with each PP2A holoenzyme, they had no impact upon the stoichiometry of PP2A subunits precipitating with either the regulatory or the scaffolding subunits. We conclude that the PP1 docking site mutations do not alter the integrity of the PP2A-B55 or PP2A-B56 holoenzyme complexes. The ability to detect S377/S378 phosphorylation in A^{Paa1} precipitates consolidates the data in Extended Data Figure 5g to demonstrate that this site between the two elements of the PP1 docking site of B56^{Par1} can be phosphorylated in the PP2A-B56^{Par1} holoenzyme complexes. Catalytic C^{Ppa1} and C^{Ppa2} and the scaffolding A^{Paa1} subunits of PP2A were detected with commercial antibodies. d) The tandem affinity purification scheme used to isolate PP2A phosphatases from yeast cultures via the TAP tag fused to the scaffolding A^{Paa1} subunit. e) Coomassie stained 4 – 12 % SDS NUPAGE gradient gels of Paa1.TAP purifications of the indicated strains. The disappearance of bands upon gene deletion combines with Mass spectrometric analysis of isolated bands after a further round of purification (Extended Data Figure 5b,c) to confirm that this procedure isolates PP2A enzymes. The persistence of the wild type pattern in *B55^{pab1}.PDSN*, *B56^{par1}.PDSN* and *B56^{par1}.S378A* strains indicates that these mutations do not alter the composition of either PP2A holoenzyme. i.e. they are not altering the structural bonds that maintain the integrity of the PP2A holo-enzyme complexes as predicted from existing current crystal structures of PP2A holoenzyme complexes[28-30].

Supplementary Material

Refer to Web version on PubMed Central for supplementary material.

Acknowledgements

This work was supported by Cancer Research UK [CRUK] Grant numbers; C147/A6058 and C29/A13678. We thank: Isabel Alvarez-Tabares (CRUK Manchester Institute), Karim Labib (Dundee University, UK), Keith Gull (University of Oxford, UK) Mitsuhiro Yanagida (OIST Okinawa, Japan), Viesturs Simanis (EPFL-ISREC, Switzerland), Jurg Bähler (UCL, UK) and Kathy Gould (Vanderbuilt University, USA) for reagents.

References

1. Wu JQ, Guo JY, Tang W, Yang CS, Freel CD, Chen C, Nairn AC, Kornbluth S. PP1-mediated dephosphorylation of phosphoproteins at mitotic exit is controlled by inhibitor-1 and PP1 phosphorylation. Nature cell biology. 2009; 11:644–651. doi:10.1038/ncb1871. [PubMed: 19396163]
2. Ohkura H, Kinoshita N, Miyatani S, Toda T, Yanagida M. The Fission Yeast *dis2*$^{+}$ Gene Required For Chromosome Disjoining Encodes One Of 2 Putative Type-1 Protein Phosphatases. Cell. 1989; 57:997–1007. [PubMed: 2544298]
3. Mochida S, Hunt T. Calcineurin is required to release Xenopus egg extracts from meiotic M phase. Nature. 2007; 449:336–340. doi:10.1038/nature06121. [PubMed: 17882219]
4. Mochida S, Ikeo S, Gannon J, Hunt T. Regulated activity of PP2A-B55 delta is crucial for controlling entry into and exit from mitosis in Xenopus egg extracts. EMBO J. 2009; 28:2777–2785. [PubMed: 19696736]
5. Schmitz MH, Held M, Janssens V, Hutchins JR, Hudecz O, Ivanova E, Goris J, Trinkle-Mulcahy L, Lamond AI, Poser I, Hyman AA, Mechtler K, Peters JM, Gerlich DW. Live-cell imaging RNAi

screen identifies PP2A-B55alpha and importin-beta1 as key mitotic exit regulators in human cells. Nature cell biology. 2010; 12:886–893. doi:10.1038/ncb2092. [PubMed: 20711181]

6. Qian J, Winkler C, Bollen M. 4D-networking by mitotic phosphatases. Current opinion in cell biology. 2013; 25:697–703. doi:10.1016/j.ceb.2013.06.005. [PubMed: 23849679]
7. Dohadwala M, da Cruz e Silva EF, Hall FL, Williams RT, Carbonaro-Hall DA, Nairn AC, Greengard P, Berndt N. Phosphorylation and inactivation of protein phosphatase 1 by cyclin-dependent kinases. Proceedings of the National Academy of Sciences of the United States of America. 1994; 91:6408–6412. [PubMed: 8022797]
8. Kwon YG, Lee SY, Choi Y, Greengard P, Nairn AC. Cell cycledependent phosphorylation of mammalian protein phosphatase 1 by cdc2 kinase. Proceedings of the National Academy of Sciences of the United States of America. 1997; 94:2168–2173. [PubMed: 9122166]
9. Yamano H, Ishii K, Yanagida M. Phosphorylation Of Dis2 Protein Phosphatase At the C-Terminal Cdc2 Consensus and Its Potential Role In Cell-Cycle Regulation. Embo Journal. 1994; 13:5310–5318. [PubMed: 7957097]
10. Ishii K, Kumada K, Toda T, Yanagida M. Requirement for PP1 phosphatase and 20S cyclosome/APC for the onset of anaphase is lessened by the dosage increase of a novel gene *sds23*$^{+}$ Embo Journal. 1996; 15:6629–6640. [PubMed: 8978689]
11. Bollen M, Peti W, Ragusa MJ, Beullens M. The extended PP1 toolkit: designed to create specificity. Trends in biochemical sciences. 2010; 35:450–458. doi:10.1016/j.tibs.2010.03.002. [PubMed: 20399103]
12. Heroes E, Lesage B, Gornemann J, Beullens M, Van Meervelt L, Bollen M. The PP1 binding code: a molecular-lego strategy that governs specificity. The FEBS journal. 2012 doi:10.1111/j.1742-4658.2012.08547.x.
13. Kinoshita N, Ohkura H, Yanagida M. Distinct, Essential Roles Of Type-1 and Type-2a Protein Phosphatases In the Control Of the Fission Yeast-Cell Division Cycle. Cell. 1990; 63:405–415. [PubMed: 2170029]
14. Sents W, Ivanova E, Lambrecht C, Haesen D, Janssens V. The biogenesis of active protein phosphatase 2A holoenzymes: a tightly regulated process creating phosphatase specificity. The FEBS journal. 2013; 280:644–661. doi:10.1111/j.1742-4658.2012.08579.x. [PubMed: 22443683]
15. Kitajima TS, Sakuno T, Ishiguro K, Iemura S, Natsume T, Kawashima SA, Watanabe Y. Shugoshin collaborates with protein phosphatase 2A to protect cohesin. Nature. 2006; 441:46–52. doi:10.1038/nature04663. [PubMed: 16541025]
16. Suijkerbuijk SJ, Vleugel M, Teixeira A, Kops GJ. Integration of kinase and phosphatase activities by BUBR1 ensures formation of stable kinetochore-microtubule attachments. Developmental cell. 2012; 23:745–755. doi:10.1016/j.devcel.2012.09.005. [PubMed: 23079597]
17. Kinoshita K, Nemoto T, Nabeshima K, Kondoh H, Niwa H, Yanagida M. The Regulatory Subunits Of Fission Yeast Protein Phosphatase 2A (PP2A) Affect Cell Morphogenesis, Cell-Wall Synthesis and Cytokinesis. Genes to Cells. 1996; 1:29–45. [PubMed: 9078365]
18. Jiang W, Hallberg RL. Isolation and characterization of *par1*$^{+}$ and *par2*$^{+}$: two *Schizosaccharomyces pombe* genes encoding B' subunits of protein phosphatase 2A. Genetics. 2000; 154:1025–1038. [PubMed: 10757751]
19. Alvarez-Tabares I, Grallert A, Ortiz JM, Hagan IM. *Schizosaccharomyces pombe* protein phosphatase 1 in mitosis, endocytosis and a partnership with Wsh3/Tea4 to control polarised growth. J Cell Sci. 2007; 120:3589–3601. [PubMed: 17895368]
20. Grallert A, Chan KY, Alonso-Nunez ML, Madrid M, Biswas A, Alvarez-Tabares I, Connolly Y, Tanaka K, Robertson A, Ortiz JM, Smith DL, Hagan IM. Removal of Centrosomal PP1 by NIMA Kinase Unlocks the MPF Feedback Loop to Promote Mitotic Commitment in *S. pombe*. Current biology : CB. 2013; 23:213–222. doi:10.1016/j.cub.2012.12.039. [PubMed: 23333317]
21. King SM, Hyams JS. Synchronization Of Mitosis In a Cell-Division Cycle Mutant Of *Schizosaccharomyces pombe* Released From Temperature Arrest. Canadian Journal Of Microbiology. 1982; 28:261–264.
22. Ishiguro T, Tanaka K, Sakuno T, Watanabe Y. Shugoshin-PP2A counteracts casein-kinase-1-dependent cleavage of Rec8 by separase. Nature cell biology. 2010; 12:500–506. doi:10.1038/ncb2052. [PubMed: 20383139]

23. Johnson LN. Substrates of mitotic kinases. Science signaling. 2011; 4:pe31. doi:10.1126/scisignal.2002234. [PubMed: 21712544]
24. Janssens V, Longin S, Goris J. PP2A holoenzyme assembly: in cauda venenum (the sting is in the tail). Trends in biochemical sciences. 2008; 33:113–121. doi:10.1016/j.tibs.2007.12.004. [PubMed: 18291659]
25. Porter IM, Schleicher K, Porter M, Swedlow JR. Bod1 regulates protein phosphatase 2A at mitotic kinetochores. Nature communications. 2013; 4:2677. doi:10.1038/ncomms3677.
26. Pines J, Hagan I. The Renaissance or the cuckoo clock. Philosophical transactions of the Royal Society of London. Series B. Biological sciences. 2011; 366:3625–3634. doi:10.1098/rstb.2011.0080. [PubMed: 22084388]
27. Kim Y, Holland AJ, Lan W, Cleveland DW. Aurora kinases and protein phosphatase 1 mediate chromosome congression through regulation of CENP-E. Cell. 2010; 142:444–455. doi:10.1016/j.cell.2010.06.039. [PubMed: 20691903]
28. Xu Y, Xing Y, Chen Y, Chao Y, Lin Z, Fan E, Yu JW, Strack S, Jeffrey PD, Shi Y. Structure of the protein phosphatase 2A holoenzyme. Cell. 2006; 127:1239–1251. doi:10.1016/j.cell.2006.11.033. [PubMed: 17174897]
29. Cho US, Xu W. Crystal structure of a protein phosphatase 2A heterotrimeric holoenzyme. Nature. 2007; 445:53–57. doi:10.1038/nature05351. [PubMed: 17086192]
30. Xu Y, Chen Y, Zhang P, Jeffrey PD, Shi Y. Structure of a protein phosphatase 2A holoenzyme: insights into B55-mediated Tau dephosphorylation. Molecular cell. 2008; 31:873–885. doi:10.1016/j.molcel.2008.08.006. [PubMed: 18922469]
31. Moreno S, Klar A, Nurse P. Molecular genetic analysis of fission yeast *Schizosaccharomyces pombe*. Methods In Enzymology. 1991; 194:795–823. [PubMed: 2005825]
32. Fennessy D, Grallert A, Krapp A, Cokoja A, Bridge AJ, Petersen J, Patel A, Tallada VA, Boke E, Hodgson B, Simanis V, Hagan IM. Extending the *Schizosaccharomyces pombe* Molecular Genetic Toolbox. PloS one. 2014; 9:e97683. doi:10.1371/journal.pone.0097683. [PubMed: 24848109]
33. Creanor J, Mitchison JM. Reduction of perturbations in leucine incorporation in synchronous cultures of *Schizosaccharomyces pombe* made by elutriation. Journal of General Microbiology. 1979; 112:385–388.
34. Qian J, Lesage B, Beullens M, Van Eynde A, Bollen M. PP1/Repo-man dephosphorylates mitotic histone H3 at T3 and regulates chromosomal aurora B targeting. Current biology : CB. 2011; 21:766–773. doi:10.1016/j.cub.2011.03.047. [PubMed: 21514157]
35. Petersen J, Paris J, Willer M, Philippe M, Hagan IM. The *S. pombe* aurora related kinase Ark1 associates with mitotic structures in a stage dependent manner and is required for chromosome segregation. Journal of Cell Science. 2001; 114:4371–4384. [PubMed: 11792803]
36. Hagan I, Yanagida M. Novel potential mitotic motor protein encoded by the fission yeast *cut7*$^{+}$ gene. Nature. 1990; 347:563–566. [PubMed: 2145514]
37. Gould KL, Ren L, Feoktistova AS, Jennings JL, Link AJ. Tandem affinity purification and identification of protein complex components. Methods. 2004; 33:239–244. doi:10.1016/j.ymeth.2003.11.019. [PubMed: 15157891]
38. Mansfeld J, Collin P, Collins MO, Choudhary JS, Pines J. APC15 drives the turnover of MCC-CDC20 to make the spindle assembly checkpoint responsive to kinetochore attachment. Nature cell biology. 2011; 13:1234–1243. doi:10.1038/ncb2347. [PubMed: 21926987]
39. Beullens M, Van Eynde A, Vulsteke V, Connor J, Shenolikar S, Stalmans W, Bollen M. Molecular determinants of nuclear protein phosphatase-1 regulation by NIPP-1. The Journal of biological chemistry. 1999; 274:14053–14061. [PubMed: 10318819]
40. Gordon C, McGurk G, Wallace M, Hastie ND. A Conditional-Lethal Mutant In the Fission Yeast 26-S Protease Subunit Mts3(+) Is Defective In Metaphase to Anaphase Transition. Journal Of Biological Chemistry. 1996; 271:5704–5711. [PubMed: 8621436]
41. Gambus A, Jones RC, Sanchez-Diaz A, Kanemaki M, van Deursen F, Edmondson RD, Labib K. GINS maintains association of Cdc45 with MCM in replisome progression complexes at eukaryotic DNA replication forks. Nature cell biology. 2006; 8:358–366. doi:10.1038/ncb1382. [PubMed: 16531994]

42. Hachet O, Berthelot-Grosjean M, Kokkoris K, Vincenzetti V, Moosbrugger J, Martin SG. A phosphorylation cycle shapes gradients of the DYRK family kinase Pom1 at the plasma membrane. Cell. 2011; 145:1116–1128. doi:10.1016/j.cell.2011.05.014. [PubMed: 21703453]

43. Nurse P. Universal control mechanism regulating onset of M-phase. Nature. 1990; 344:503–508. [PubMed: 2138713]

44. Hudson JD, Feilotter H, Young PG. *stf1*: non wee mutations epistatic to *cdc25* in the fission yeast *Schizosaccharomyces pombe*. Genetics. 1990; 126:309–315. [PubMed: 2245912]

45. Ishihama Y, Oda Y, Tabata T, Sato T, Nagasu T, Rappsilber J, Mann M. Exponentially modified protein abundance index (emPAI) for estimation of absolute protein amount in proteomics by the number of sequenced peptides per protein. Molecular & cellular proteomics : MCP. 2005; 4:1265–1272. doi:10.1074/mcp.M500061-MCP200. [PubMed: 15958392]

46. Ohkura H, Yanagida M. *S. pombe* Gene $sds22^{+}$ Essential For a Midmitotic Transition Encodes a Leucine-Rich Repeat Protein That Positively Modulates Protein Phosphatase-1. Cell. 1991; 64:149–157. [PubMed: 1846086]

47. Stone EM, Yamano H, Kinoshita N, Yanagida M. Mitotic Regulation Of Protein Phosphatases By the Fission Yeast Sds22-Protein. Current Biology. 1993; 3:13–26. [PubMed: 15335873]

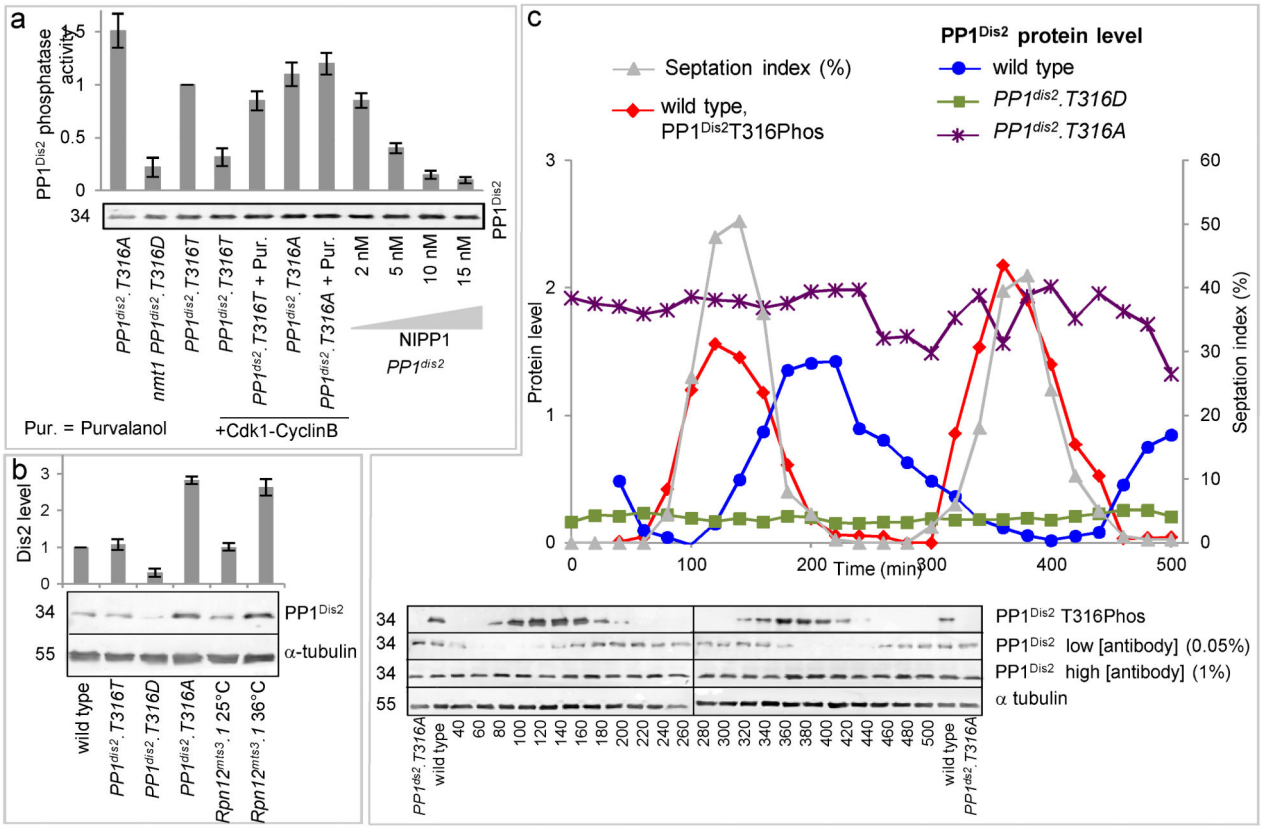

Figure 1. PP1^{Dis2} threonine 316 phosphorylation and stability

a) EnzChek phosphatase assays (Extended data Figure 1b) of PP1^{Dis2} isolated from the indicated strains by antibody precipitation. "+ Cdk1-Cyclin B" indicates the addition of sepharose beads to which covalently linked p13^{Suc1} protein had recruited Cdk1-Cyclin B from *S. pombe* cell extracts. NIPP1 is a highly specific PP1 inhibitor. Purvalanol is a Cdk1 inhibitor. b, c) PP1^{Dis2} and T316 phosphorylation levels (*Rpn12^{mts3}.1* is a temperature sensitive proteasome mutation). For b,c) n=5; Bars=standard deviation c) Size selected cells transit the cell division cycle. The septation profile is for the wild type culture. Dis2.T316D and Dis2.T316A levels from the experiments in Extended Data Figures 1f,g are superimposed on this wild type dataset.

Europe PMC Funders Author Manuscripts

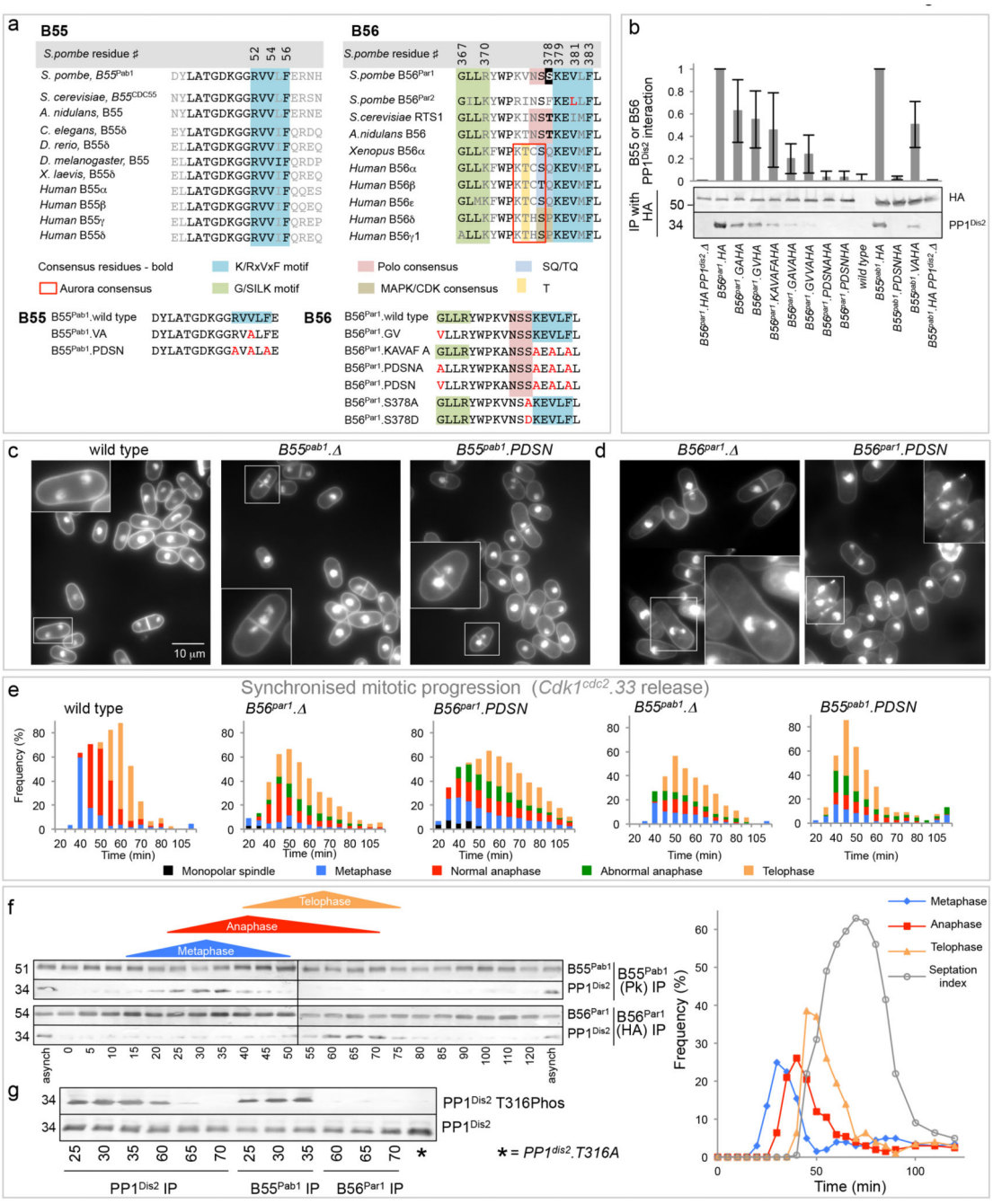

Figure 2. PP1^{Dis2} recruitment to PP2A-B55^{Pab1} and PP2A-B56^{Par1} regulates chromosome segregation

a) Clustal W alignments of PP1 docking motifs in B55 and B56 molecules. b,f,g) Immunoprecipitation reactions probed with PP1^{Dis2} [20] and T316Phos polyclonal and 12CA5 and 366 monoclonal (HA and Pk epitopes respectively) antibodies. For f, mitotic progression was scored by tubulin staining with “Telophase” defined by post-anaphase arrays of microtubules. For b) n=6, bars=standard deviation. c,d) DAPI staining. e) Tubulin

Europe PMC Funders Author Manuscripts

immunofluorescence staining for *Cdk1*^{cdc2}*.33* “arrest release” experiments scored mitotic progression.

Europe PMC Funders Author Manuscripts

Europe PMC Funders Author Manuscripts

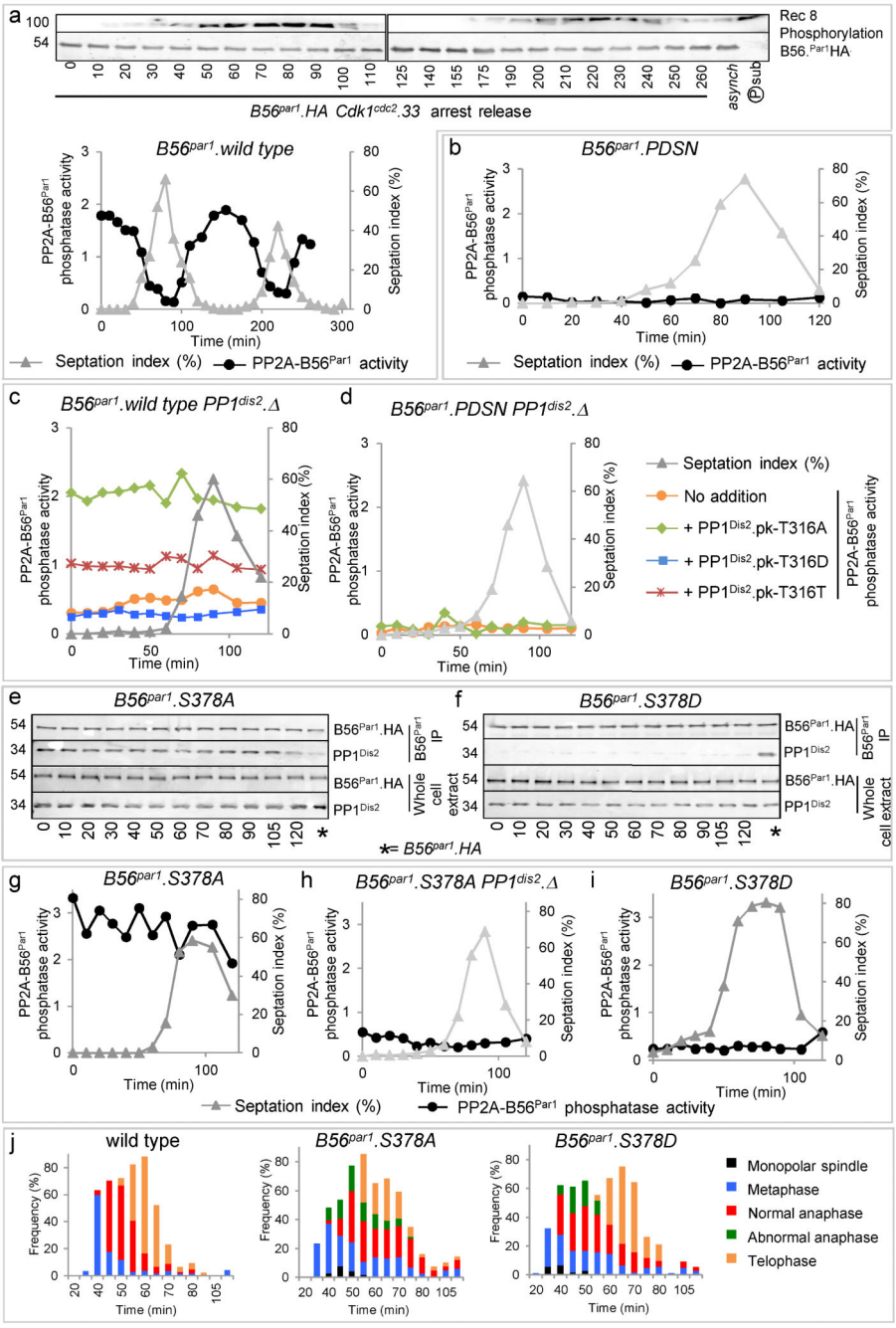

Figure 3. Phosphorlyation status of serine 378 determines competence to recruit active PP1^{Dis2} to PP2A-B56^{Par1} to promote PP2A-B56^{Par1} activity

Assays of PP2A-B56^{Par1} activity following B56^{Par1}.HA immunoprecipitation (with 12CA5 antibodies) of *Cdk1^{cdc2}.33* arrest release synchronised cultures followed for one (b, g-i) or two (a) cycles. Activity changes (loss of GST-Rec8$^{391-561}$ ^{32}P radioactivity[22]) at each point were normalised to the activity of B56^{Par1}.HA from an asynchronous culture processed in parallel on the same gel (penultimate lane). (c,d) Aliquots of PP1^{Dis2} protein immunoprecipitates (isolated under high salt (1.2M NaCl) extraction conditions to

disassociate partners) from *Cdk1*^{cdc2}*.33* arrested (interphase) cultures were added to PP2A-B56^{Par1} assays from *Cdk1*^{cdc2}*.33 dis2*.Δ cultures (Extended Data Figure 6). (e,f) Co-immunoprecipitation assays as for Figure 2b. (j) Phenotype analysis of *Cdk1*^{cdc2}*.33* synchronised mitoses as for Figure 2e.

Europe PMC Funders Author Manuscripts

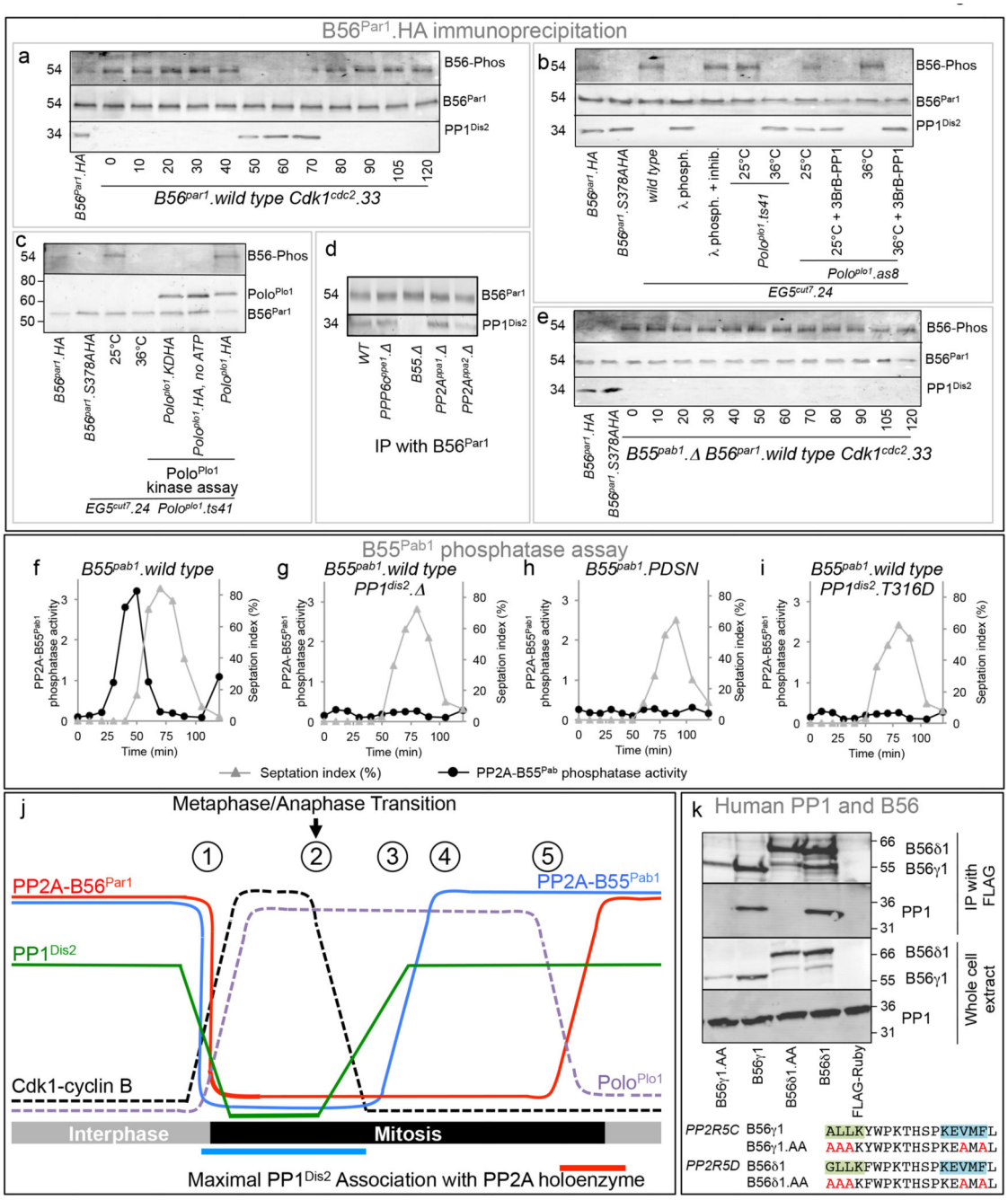

Figure 4. The mitotic phosphatase relay: PP2A-B55^{Pab1} de-phosphorylation of B56^{Par1} promotes PP1^{Dis2} recruitment to activate PP2A-B56^{Par1} phosphatase

a, e-i) *Cdk1^{cdc2}.33* synchronised mitoses. a-c, e) B56-Phos antibodies (Extended Data Figure 7a) detected phosphorylation on B56^{Par1} following immunoprecipitation from the indicated strains and the indicated treatments. PP1^{Dis2} levels were monitored where indicated. *Polo^{Plo1}.KDHA* = HA tagged catalytically inactive. d) B56^{Par1} precipitates probed for PP1^{Dis2}. f-i) PP2A-B55^{Pab1} phosphatase assays (Extended Data Figure 7c-f). j) Bulk activities are illustrated: local activities at any given time will depend on the specific balance

Europe PMC Funders Author Manuscripts

of each activity at a particular site. 1) Cdk1-CyclinB activation represses all three phosphatase activities (Extended Data Figure 9a). Direct phosphorylation of $PP1^{Dis2}$ TPRR motif inhibits catalytic activity[1,7-10] and promotes destruction. $PP1^{Dis2}$ binds $B55^{Pab1}$ but cannot reactivate PP2A-$B55^{Pab1}$ while TPRR phosphorylation persists. $Polo^{Plo1}$ phosphorylation of $B56^{Par1}$ prevents $PP1^{Dis2}$ recruitment to PP2A-$B56^{Par1}$. 2) Declining Cdk1-Cyclin B activity facilitates PP1 auto-reactivation. 3) Re-activated $PP1^{Dis2}$ promotes PP2A-$B55^{Pab1}$ reactivation. 4) PP2A-$B55^{Pab1}$ de-phosphorylates the PP1 docking site in $B56^{Par1}$ less efficiently than $Polo^{Plo1}$ phosphorylates it to keep PP2A-$B56^{Par1}$ activity low. 5) Declining $Polo^{Plo1}$ activity enables PP2A-$B55^{Pab1}$ to dephosphorylate $B56^{Par1}$ and promote reactivating recruitment of $PP1^{Dis2}$ (Extended Data Figure 8). k) Flag tagged B56γ and B56δ isoforms were stably expressed in HeLa-FRT cell lines, immunoprecipitated from mitotic cells isolated by shake-off from nocodazoletreated cells, and the immunoprecipitates probed with an antibody that recognises all forms of PP1.

Europe PMC Funders Author Manuscripts